1997-06

Propagation of vertically polarized waves over rough ocean surfaces

Conrad, Jeffrey G

Monterey, California. Naval Postgraduate School

NAVAL POSTGRADUATE SCHOOL
MONTEREY, CALIFORNIA

THESIS

PROPAGATION OF VERTICALLY POLARIZED WAVES OVER ROUGH OCEAN SURFACES

by

Jeffrey G. Conrad

June 1997

Thesis Advisor: Ramakrishna Janaswamy
Second Reader: David C. Jenn

Approved for public release; distribution is unlimited.

REPORT DOCUMENTATION PAGE

Form Approved OMB No. 0704-0188

1. AGENCY USE ONLY *(Leave blank)*	2. REPORT DATE	3. REPORT TYPE AND DATES COVERED
	June 1997	Master's Thesis

4. TITLE AND SUBTITLE PROPAGATION OF VERTICALLY POLARIZED WAVES OVER ROUGH OCEAN SURFACES	5. FUNDING NUMBERS
6. AUTHOR(S) Jeffrey G. Conrad	
7. PERFORMING ORGANIZATION NAME(S) AND ADDRESS(ES) Naval Postgraduate School Monterey, CA 93943-5000	8. PERFORMING ORGANIZATION REPORT NUMBER
9. SPONSORING/MONITORING AGENCY NAME(S) AND ADDRESS(ES)	10. SPONSORING/MONITORING AGENCY REPORT NUMBER

11. SUPPLEMENTARY NOTES The views expressed in this thesis are those of the author and do not reflect the official policy or position of the Department of Defense or the U.S. Government.

12a. DISTRIBUTION/AVAILABILITY STATEMENT Approved for public release; distribution is unlimited.	12b. DISTRIBUTION CODE

13. ABSTRACT *(maximum 200 words)*

The problem of propagation of vertically polarized radiowaves in an inhomogeneous atmosphere and over rough ocean surfaces is solved using the parabolic equation method. The solution of the parabolic equation is accomplished through the use of the Fourier split-step algorithm. Formulation of the equations is based upon (i) recognizing that the Fourier kernels of the transform equations in the split step algorithm represent planes waves and (ii) compensating for the effects of rough ocean surfaces by using a rough surface reduction factor directly in the spectral domain. To accomplish this a redefinition of the Fourier transform pair is done to ensure mathematical consistency. The formulation also incorporates the first and second derivatives of the refractivity index to accommodate steep gradients in the refractivity profile. Hanning windows are used in both the spatial and wavenumber domains to contain computational requirements. The effects on propagation by varying parameters such as wave heights, computational domain ceilings, frequency and step size are investigated.

14. SUBJECT TERMS Radio Wave Propagation, Parabolic Equation, Rough Ocean Surface, Fourier Split-step Algorithm.	15. NUMBER OF PAGES 57
	16. PRICE CODE

17. SECURITY CLASSIFICATION OF REPORT	18. SECURITY CLASSIFICATION OF THIS PAGE	19. SECURITY CLASSIFICATION OF ABSTRACT	20. LIMITATION OF ABSTRACT
Unclassified	Unclassified	Unclassified	UL

NSN 7540-01-280-5500

Standard Form 298 (Rev. 2-89)
Prescribed by ANSI Std. 239-18 298-102

Approved for public release; distribution is unlimited.

PROPAGATION OF VERTICALLY POLARIZED WAVES OVER ROUGH OCEAN SURFACES

Jeffrey G. Conrad
Lieutenant-Commander, Canadian Navy
BSc., Dalhousie University, 1985

Submitted in partial fulfillment
of the requirements for the degree of

MASTER OF SCIENCE
IN
ELECTRICAL AND COMPUTER ENGINEERING

from the

NAVAL POSTGRADUATE SCHOOL
June 1997

ABSTRACT

The problem of propagation of vertically polarized radiowaves in an inhomogeneous atmosphere and over rough ocean surfaces is solved using the parabolic equation method. The solution of the parabolic equation is accomplished through the use of the Fourier split-step algorithm. Formulation of the equations is based upon (i) recognizing that the Fourier kernels of the transform equations in the split step algorithm represent planes waves and (ii) compensating for the effects of rough ocean surfaces by using a rough surface reduction factor directly in the spectral domain. To accomplish this a redefinition of the Fourier transform pair is done to ensure mathematical consistency. The formulation also incorporates the first and second derivatives of the refractivity index to accommodate steep gradients in the refractivity profile. Hanning windows are used in both the spatial and wavenumber domains to contain computational requirements. The effects on propagation by varying parameters such as wave heights, computational domain ceilings, frequency and step size are investigated.

TABLE OF CONTENTS

LIST OF FIGURES

LIST OF TABLES

I. INTRODUCTION

A. BACKGROUND

Propagation of radiowaves over rough ocean surfaces and in an inhomogeneous atmosphere is a topic of particular interest to the Navy. The effects of this type of environment on the strength of a signal at a given distance downrange from a transmitter are significant, and play a critical role in determining if a communication link can be successfully established, or a target can be detected by radar. This type of radiowave propagation is governed by a modified Helmholtz equation which is an elliptic partial differential equation. Solving this type of equation is computationally very intensive and becomes impractical when addressing typical propagation problems. The Helmholtz equation can be approximated by a parabolic equation (PE) if only one way propagation is considered, which is a reasonable assumption for most typical propagation problems. The advantage of using the parabolic equation approach is that a solution can be obtained much more efficiently through the use of a range stepping technique. Kuttler and Dockery [3] discuss the basic idea and various approximations involved in the development of the PE. This technique makes it possible to easily estimate propagation losses several hundreds of kilometers downrange with antenna heights up to several hundreds of meters for frequencies through the Super High Frequency (SHF) band. By only considering waves propagating in the forward direction, the strength of a signal at a given location downrange will be determined by direct and reflected (from the ocean surface) waves. Interference between these two waves will result in reflection multipath fading which can result in high gain or severe loss of signal. The effects of reflection multipath fading will depend greatly upon the surface height deviations of the ocean surface which will be determined by wind speed.

B. OBJECTIVE

In this thesis the split-step PE algorithm is used to predict propagation of vertically polarized radiowaves over rough ocean surfaces in the presence of an inhomogeneous atmosphere. This thesis builds upon work previously done by Janaswamy [1] in this area which addressed horizontal polarization. In this approach the Fourier transform pair used in the split-step PE algorithm is modified to accommodate the effects of sea surface roughness directly into the formulation. The idea behind this approach will be to cast the transform equations in terms of incident and reflected waves, and then use the rough surface reduction factor available for plane waves, according to Miller [2], directly in the spectral domain. Chapter II presents the derivation and formulation of the modified Fourier transform pair for the split-step PE algorithm. Chapter III details the generation of the numerical procedure for solving the parabolic equation. In Chapter IV the performance of the numerical solution is examined by varying several important parameters and observing the effects on radiowave propagation. The effects of changing parameters such as step size, atmospheric refractivity profile, number of points for Fast Fourier Transform (FFTs), frequency, and wind speed will be investigated. Recommendations and conclusions are presented in Chapter V.

II. FORMULATION

In this chapter we present the theory governing the parabolic equation and the derivation of the Fourier transform pair to be used with the split-step algorithm. This derivation parallels that given by Janaswamy [1] which considered the same propagation problem discussed here, but for horizontally polarized radiowaves. This chapter reiterates many of the formulas from that report but modifies them as appropriate to derive correct formulas for the case of vertically polarized waves.

Figure 1 illustrates the basic geometry of the problem we are investigating. We consider the source at an initial range ($x = 0$) and height ($z = z_t$) to be an omnidirectional point source. Given the position of the receiver, frequency of operation, refractive index profile of the atmosphere, wind speed, and the ground constants (ε_r and σ), we wish to determine the signal strength along the path between the transmitter and receiver.

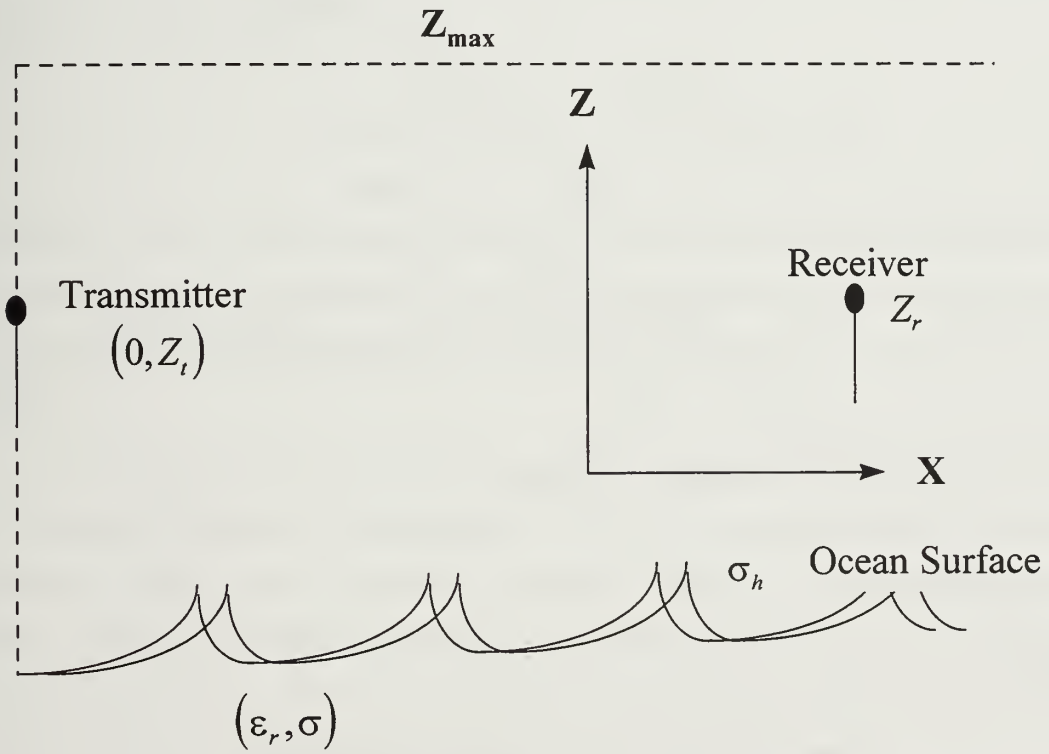

Figure 1. Source Producing Fields Over Rough Ocean Surface

To solve this propagation problem the standard parabolic equation as defined below by Kuttler and Dockery [3] is used:

$$\frac{\partial^2 u(x,z)}{\partial z^2} + 2ik_0 \frac{\partial u(x,z)}{\partial x} + 2k_0^2\left[m(x,z)-1\right]u(x,z) = 0 \ , \qquad \textbf{(1)}$$

where $u(x,z) = \sqrt{\frac{r\sin\theta}{\varepsilon(r,\theta)}} H_\phi(r,\theta)$ refers to a spherical coordinate reference system. $H_\phi(r,\theta)$ is the ϕ-component of the magnetic field. Equation (1) assumes an $e^{-i\omega t}$ time dependence. The coordinate system used in this thesis is shown in Figure 2 below.

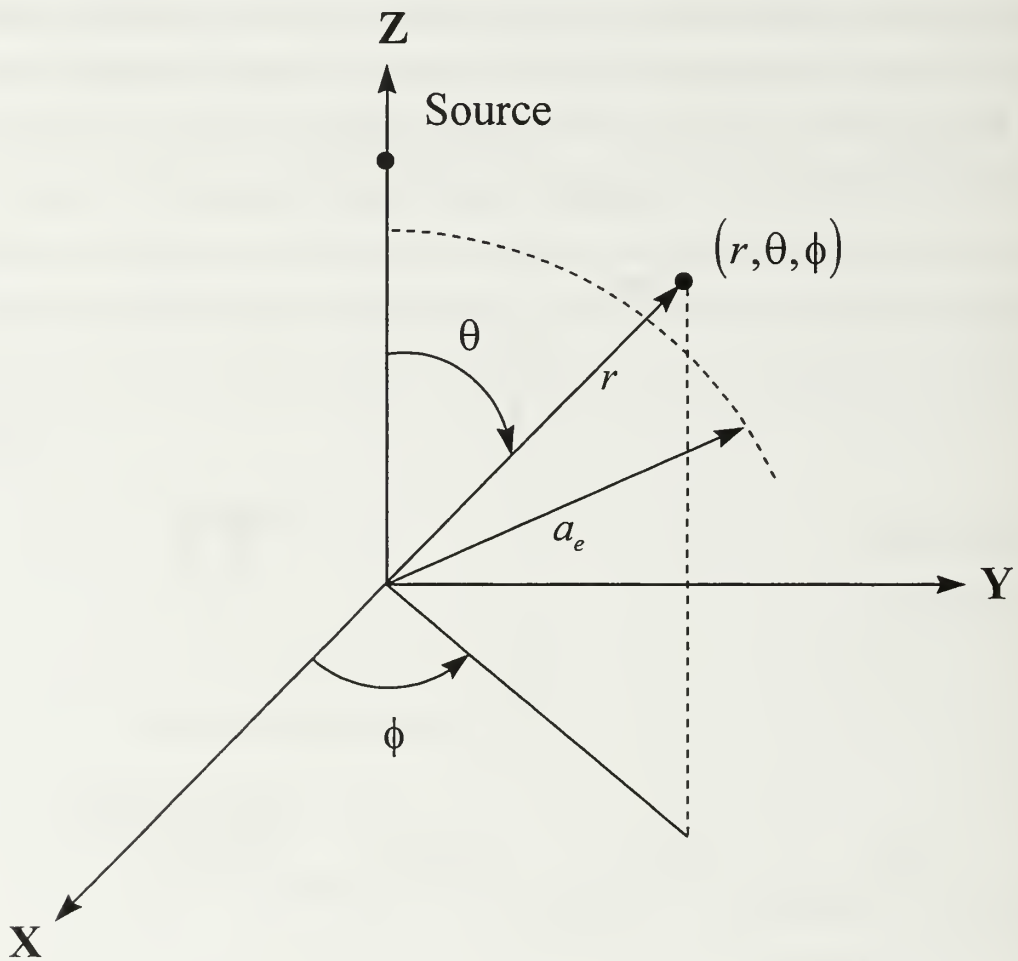

Figure 2. Earth Centered Spherical Geometry

In this coordinate system the transmitter is located at $\theta = 0$ and $r = a_e + z_t$, where a_e is the radius of the earth and z_t is the height of the transmitter above the surface of the earth. The free space wave number is given by $k_0 = \omega\sqrt{\varepsilon_0\mu_0}$, x is the range axis, z is the height axis and $m(x,z)$ is the modified refractive index under earth flattened conditions as given by Kuttler and Dockery [3] and is equal to: $m(x,z) = \frac{n+z}{a_e}$, with n being the actual refractive index.

By examining (1) we can see that the highest derivative in terms of the range, x, is of the first order for the parabolic case, unlike a Helmholtz equation which would be of second order. This desirable characteristic of the parabolic equation allows us to use (1) to solve for a field at a given range based upon a known field at a previous range. If the range step size, or Δx, is kept reasonably small and the refractive index varies slowly, the field at a new range can be computed from the field at a previous range by using the split-step algorithm by Tappert [4] below:

$$u(x,z) = e^{ik_0(m-1)\Delta x}\mathbf{F}^{-1}\left\{e^{\frac{-ip^2\Delta x}{2k_0}}\mathbf{F}\left[u(x_0,z)\right]\right\}. \qquad (2)$$

Later in this thesis we will modify this equation to accommodate refractive indices which have steep gradients. **F** represents the forward Fourier transform operator corresponding to an appropriate spectral decomposition of the field in the vertical direction, and $\mathbf{F}^{-1}$ is its inverse.

To develop the form for the Fourier operators to be used in the split-step algorithm for rough ocean surfaces it is logical to first solve for the smooth surface case, and then modify this result so it can be applied to a rough ocean surface. In our formulation the ocean surface shows up as a boundary condition for which the parabolic equation must be solved. For the smooth ocean surface case the parabolic equation as given at (1) must be solved subject to the impedance boundary:

$$\frac{\partial u(x,0)}{\partial z} + \alpha_0 u(x,0) = 0 \ , \tag{3}$$

where $\alpha_0 = \dfrac{ik_0\sqrt{\varepsilon_{rc} - 1}}{\varepsilon_{rc}}$. The complex dielectric constant, $\varepsilon_{rc,}$ is defined as:

$$\varepsilon_{rc} = \varepsilon_r + i\sigma_r \ , \tag{4}$$

where, σ_r is the relative conductivity of the earth given by:

$$\sigma_r = \frac{\sigma}{\omega\varepsilon_0} \ , \quad \omega = \text{angular frequency (rads / s)} \ . \tag{5}$$

The boundary condition given at (3) is valid only for $|\varepsilon_{rc}| >> 1$, which for ocean surfaces is easily met. To solve the standard parabolic equation given at (1) subject to the boundary condition at (4), the following mixed Fourier transform pair by Kuttler and Dockery is used [3]:

$$\tilde{u}(x,p) = \mathbf{F}_s(u) = \int_0^\infty u(x,z)\left[\alpha_0 \sin(pz) - p\cos(pz)\right]dz \ , \tag{6a}$$

$$u(x,z) = \mathbf{F}_s^{-1}(\tilde{u}) = \frac{2}{\pi}\int_0^\infty \tilde{u}(x,p)\frac{\alpha_0 \sin(pz) - p\cos(pz)}{\alpha_0^2 + p^2}dp + S(x)e^{-\alpha_0 z} \ . \tag{6b}$$

The subscript, *s*, stands for the smooth surface case and the last term in (6b), which represents a surface wave, decays with range and height and can be ignored for frequencies over 10 MHz according to Kuttler and Dockery [3], which will be the case for our work here. To better illustrate the fact this formula represents plane waves which are traveling towards and away from the boundary, it is rewritten in the mathematically equivalent form shown below:

$$\tilde{u}(x,p) = \mathbf{F}_s(\tilde{u}) = \int_0^\infty u(x,z)e^{ipz}dz + \frac{1}{\Gamma_s(p)}\int_0^\infty u(x,z)e^{-ipz}dz \ , \tag{7a}$$

$$u(x,z) = \mathbf{F}_s(\tilde{u}) = \frac{2}{\pi}\int_0^\infty \tilde{u}(x,p)\left[e^{-ipz} + \Gamma_s(p)e^{ipz}\right]dp \ , \qquad \textbf{(7b)}$$

where, $\Gamma_s(p) = \dfrac{p+i\alpha_0}{p-i\alpha_0}$, $p > 0$, represents the plane wave reflection coefficient for smooth earth. From examination of (7b) it is apparent that the field is comprised of a wave traveling towards the boundary at $z = 0$, given by $\tilde{u}(x,p)e^{-ipz}$, and one away from the boundary at $z = 0$, given by $\Gamma_s(p)\tilde{u}(x,p)e^{ipz}$. It is evident that the reflected wave is equal to the incident wave multiplied by the reflection coefficient, which makes intuitive sense.

Now that Fourier operators have been defined for the split-step algorithm in the case of a smooth ocean surface, we want to extend our derivation to include a boundary which consists of a rough ocean surface. Previous investigation of the problem of plane wave reflection from rough surfaces has resulted in the Kirchoff approximation and the concept of a rough surface reduction factor as given by Beckmann and Spizzichino [5]. To accommodate surface roughness for our problem we simply modify the smooth surface reflection coefficient, $\Gamma_s(p)$, by multiplying it with a rough surface reduction factor (defined below) to yield a rough surface reflection coefficient, $\Gamma_r(p)$.

$$\Gamma_r(p) = \rho_0(p,\sigma_h)\Gamma_s(p) \ . \qquad \textbf{(8)}$$

The term, $\rho_o(p;\sigma_h)$, is the rough surface reduction factor and has been derived by Miller [2] as:

$$\rho_0(p,\sigma_h) = e^{-2p^2\sigma_h^2} I_0\left(2p^2\sigma_h^2\right) \ . \qquad \textbf{(9)}$$

The $I_o(\text{-})$ term in (9) is the modified Bessel function of the first kind of order zero and σ_h represents the rms wave height deviation as determined by wind speed according to the formula:

$$\sigma_h = 0.0051\mu^2 \ , \tag{10}$$

where μ = wind speed (m/s). A simpler form for the rough surface reduction factor has been recommended in CCIR report 1008-1 [6]:

$$\rho_0(p,\sigma_h) \cong \frac{1}{\sqrt{3.2X - 2 + \sqrt{(3.2X)^2 - 7X + 9}}} \ , \tag{11}$$

where $X = 2\rho^2\sigma_h^2$.

We have now presented the necessary material to allow us to modify the Fourier operators such that the split-step algorithm can be used to predict propagation of vertically polarized waves over rough oceans surfaces. The field equation given for smooth surfaces at (7b) now becomes as follows for rough surfaces:

$$u(x,z) = \mathbf{F}_r^{-1}\left[\tilde{u}(x,p)\right] = \frac{1}{2\pi}\int_0^\infty \tilde{u}(x,p)\left[e^{-ipz} + \Gamma_r e^{ipz}\right]dp \ , \tag{12}$$

where, $\mathbf{F}_r^{-1}$, represents the inverse Fourier operator for rough surfaces. The forward transform formula requires a bit more work to develop then simply substituting Γ_r into (7a) for Γ_s (as was done for the inverse transform) as this would not satisfy the consistency requirement $\mathbf{F}\left[\mathbf{F}^{-1}(\tilde{u})\right] = \tilde{u}$. To derive the forward transform, both sides of (12) are alternately multiplied by $e^{\pm ipz}$, integrated with respect to z, and then appropriate linear combinations are taken. The result of this process yields the following for the forward Fourier transform:

$$\tilde{u}(x,p) = \int_0^\infty u(x,z)e^{ipz}dz + \frac{1}{\Gamma_r(p)}\int_0^\infty u(x,z)e^{-ipz}dz + i\int_0^\infty k(p,q)\tilde{u}(x,q)dq \ , \tag{13}$$

where the kernal $k(p,q)$ in the last integral on the right hand side is:

$$k(p,q) = \left[\frac{\Gamma_r(p) - \Gamma_r(q)}{q-p} + \frac{1 - \Gamma_r(p)\Gamma_r(q)}{q+p}\right] \cdot \frac{1}{2\pi\Gamma_r(p)} \ , \tag{14}$$

For $p = q$, a limit can be performed to yield:

$$k(p,p) = \left[-\Gamma_r'(p) + \frac{1-\Gamma_r^2(p)}{2p} \right] \cdot \frac{1}{2\pi\Gamma_r(p)} , \tag{15}$$

where $\Gamma_r'(p)$ represents the derivative of the rough surface reflection coefficient. In deriving (13), we have made use of the following identity from Papoulis [7]:

$$\int_0^\infty e^{ipz\,dz} = \pi\delta(p) + \frac{i}{p} , \tag{16}$$

where $\delta(\text{-})$ is the delta function.

Equation (13) may be rewritten in operator form by denoting the last integral on the right hand side as, $K_c\tilde{u}$ which yields:

$$\begin{aligned} \tilde{u}(x,p) &= (I - iK_c)^{-1} \left[\int_0^\infty u(x,z)e^{ipz}dz + \frac{1}{\Gamma_r(p)} \int_0^\infty u(x,z)e^{-ipz}dz \right], \\ &= \mathbf{F}_r[u(x,z)] \end{aligned} \tag{17}$$

where $\mathbf{F}_r$ represents the forward Fourier transform for rough surfaces and I is the identity operator. For notational convenience we define the quantity P:

$$P = (I - iK_c) . \tag{18}$$

III. SOLUTION PROCEDURE

In the previous chapter we presented the case for using the parabolic equation and split-step algorithm to tackle the propagation problem of vertically polarized waves over rough ocean surfaces. We then defined a consistent forward and inverse Fourier transform pair to be used with the split-step algorithm. In this chapter we explain the solution procedure using this transform pair to determine field strengths at a given range.

The solution procedure begins by recalling that we defined our transmitter source to be an omnidirectional point source at a height $z = z_t$. Numerically this initial field, u(x,z) at range $x = 0$, can be represented by a delta function. To determine the field at our first step downrange, $(x = n\Delta x)$ for $n = 1$, (17) is solved for $\tilde{u}(x,p)$ with $u(x,z)$ equal to the delta function. For this initial case, (17) becomes:

$$\tilde{u}(x,p) = (I - iK_c)^{-1}\left[e^{ipz_t} + \frac{e^{-ipz_t}}{\Gamma_r(p)}\right]. \tag{19}$$

Once the initial $\tilde{u}(x,p)$ is known the $\tilde{u}$ at the new range is determined by propagating in free space. This is represented by the term $e^{-ip^2\frac{\Delta x}{2k_0}}$ in (2). Equation (12) can then be solved for the field $u(x,z)$ at the first step downrange. A second phase correction is then applied to this field to compensate for variations in the index of refraction. This phase correction is seen as the $e^{ik_0(m-1)\Delta x}$ term in (2).While this phase correction is suitable for most environmental scenarios, it is not considered adequate for rough surfaces when severe refractive index gradients are present. For this case we include the first and second derivatives of the refractive index and then modify (2) as shown below. The first and second derivatives were determined by doing a cubic spline interpolation of the given refractivity index data. The new formula that includes higher derivatives of the refractive index is:

$$u(x,z) = e^{ik_0 m\Delta x\left((m-1)-\frac{[m'\Delta x]^2}{6}\right)-\frac{[m''\Delta x]^2}{4}} \mathbf{F}_r^{-1}\left\{e^{-ip^2\frac{\Delta x}{k_0}}\mathbf{F}_r\left[u(x_0,z)\right]\right\}, \tag{20}$$

where $\Delta x = x - x_0$. Once a solution to (20) has been determined we can now take another step downrange, $(x = n\Delta x)$ for $n = 2$, and repeat the process described above. This range stepping process continues until the field is determined at the desired distance downrange.

For a given $u(x,z)$ (17) is solved by numerically evaluating the quantity in the square brackets and then applying the inverse operator P^{-1} on it. The numerical solution was obtained using MATLAB code to compute the Fourier transforms by means of an N point complex FFT. In order to program the solution to (17) the continuous operator P first had to be put into a discrete form. This was done by using Simpson's rule with weights, S_n, to discretize the last integral in equation (13) to yield:

$$\begin{aligned} K_c\tilde{u}(x,m\Delta p) &\approx \Delta p\sum_{n=1}^{\frac{N}{2}} S_n\tilde{u}(x,n\Delta p)k(m\Delta p,n\Delta p) \\ &= K\tilde{u} \end{aligned}, \tag{21}$$

where K is of order $\left(\frac{N}{2}\times\frac{N}{2}\right)$ and is the discrete version of the continuous K_C. The upper limit in the summation is $\frac{N}{2}$ and not N because the integral is over the semi-infinite interval $[0,\infty)$, whereas the complex FFTs assume limits of $(-\infty,\infty)$. The lower limit is 1 because $\tilde{u}(x,0) = 0$. The elements of K are:

$$K_{mn} = \Delta p S_n k(m\Delta p, n\Delta p)\ ,\ m,n = 1,2,\ldots,\frac{N}{2}\ , \tag{22}$$

As mentioned above, an N-point FFT is used for the computation of the Fourier transform pair. Let us assume that the various quantities are band limited over $-p_{max} \le p \le p_{max}$, and that the transform is evaluated at $p = 0,\ \Delta p,\ 2\Delta p,\ \ldots,\ (N\text{-}1)\ \Delta p$, where:

$$\Delta p = \frac{2\pi}{N\Delta z} \quad . \tag{23}$$

Positive wavenumbers occur at $p = \Delta p, 2\Delta p, \ldots, \left(\frac{N}{2} - 1\right)\Delta p$, while negative wavenumbers occur at $\left(\frac{N}{2} + 1\right)\Delta p, \left(\frac{N}{2} + 2\right)\Delta p, \ldots, (N-1)\Delta p$. The value $\frac{N}{2}\Delta p$ corresponds to both $-p_{max}$ and p_{max}.

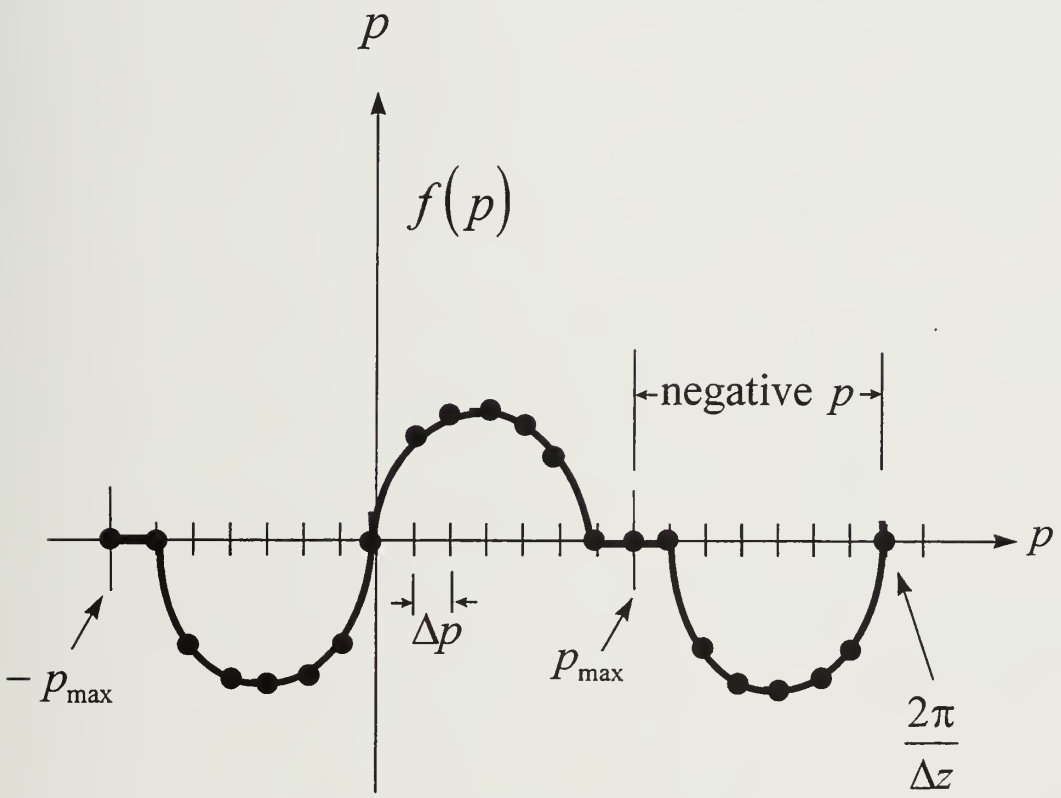

Figure 3. Wavenumber Spectrum p

To contain the computational domain vertically in the physical space, up to a maximum height z_{max}, and to bandlimit the signal in the p-space, a Hanning window is employed in both the spatial and wavenumbers domains as follows:

$$h(n) = \begin{cases} 1, & 0 \le n \le \dfrac{3N}{8} \\ \sin^2 \dfrac{4\pi n}{N}, & \dfrac{3N}{8} \le n \le \dfrac{N}{2} \end{cases}$$

Note that the Hanning window forces a gradual rolloff to zero of the data set as can be seen in Figure 4.

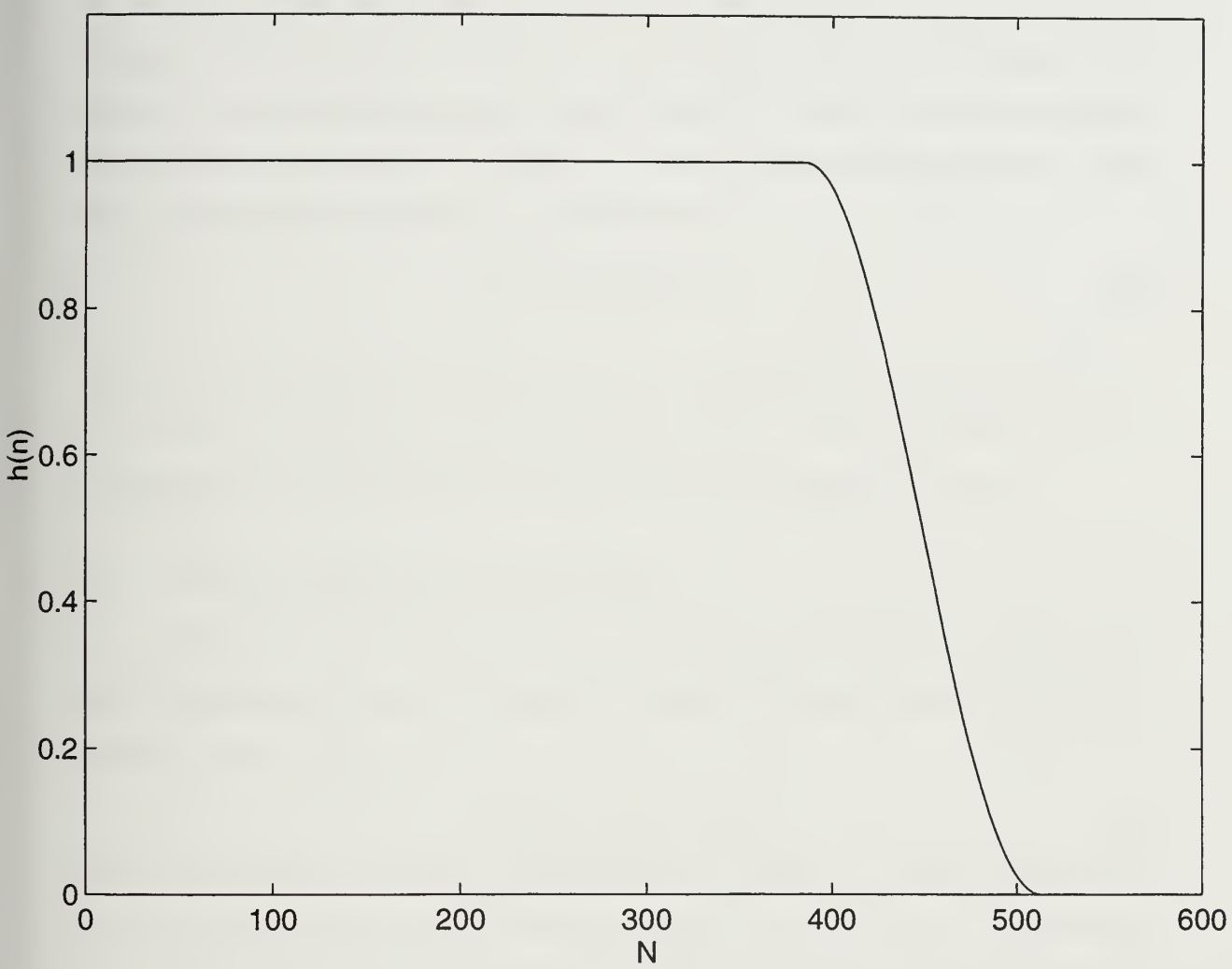

Figure 4. Hanning Window

IV. RESULTS

In Chapters I - III we presented theoretical background and described the solution procedure for using the parabolic equation and Fourier split-step algorithm to solve the problem of propagation of vertically polarized waves over rough ocean surfaces. In this chapter we present numerical results for a variety of propagation scenarios. We will investigate the effects on propagation by varying parameters such as wind speed, step size, frequency, height of the upper boundary and refractivity index profile. Throughout this chapter we present plots showing Propagation Factor (PF), in dB, versus receiver height or distance downrange, where PF is defined as excess signal over free space. For a point source, the propagation factor can be computed from:

$$\mathrm{PF} = 10\log\left(|u|^2 x\lambda_0\right) , \tag{24}$$

where x is the downrange or horizontal distance from the transmitter, u is the field, and λ_0 is the operating wavelength of the propagating signal. A positive (negative) value of propagation factor indicates a gain (loss) with respect to propagation in free space.

A. CASE 1 - STANDARD ATMOSPHERE

We begin our numerical results by running a test case against known data to validate our PE formulation. We look at propagation in standard atmosphere where the refractivity $M = (m-1)\times 10^6$ is given by:

$$M(z) = (340 + 0.118z) , \tag{25}$$

where z is the height in meters. The transmitter is at a height of z_t = 30m, horizontal step size is Δx = 200m and the ground constants are given by ε_r = 80 and σ = 4 Seimens per meter (S/m). Figure 5 shows the refractivity profile for the case of standard atmosphere. Figure 6 shows Propagation Factor versus Receiver Height at a range of 40 km with an upper boundary Z_{max} = 512m, frequency of operation = 3 GHz and N= 512. This lobing pattern compares very favorably with that given by Kuttler and Dockery [3]. Figures (7-10)

illustrate the effects of increasing wind speed and hence increasing surface roughness, for various heights of the upper boundary. Note that while the value of the upper boundary changes between Figures 7, 8 (150m) and Figures 9, 10 (300m), the vertical step size Δz remains the same (0.146m). This is so because when the height of the upper boundary was doubled the number of points, N, in our FFT also doubled. For these figures, frequency = 10 GHz, transmitter and receiver are both at a height of 25m, and Δz = 0.146m. From Figures 7 and 8 one can see that as wind speed increases the excursions of the PF in the interference region is reduced and at longer ranges the PF curve no longer decays smoothly. The departure of propagation factor from monotonous decay for large ranges is due to numerical reflections from the upper boundary. Figures 9 and 10 have an upper boundary of 300m. We can see by increasing Z_{max} (and keeping the step size Δz constant) the numerical reflections from the upper boundary do not affect the decay of the PF until further downrange.

B. CASE 2 - TRI-LINEAR DUCT

Our second case involves examining propagation where the index of refraction is characterized by a tri-linear duct as shown in Figure 11. Numerically, refractivity is given by:

$$M(z) = \begin{cases} 340 + 0.118z & 0 \le z \le 135, \\ 499.03 - 1.06z & 135 \le z \le 150, \\ 322.33 + 0.118z & z \ge 150, \end{cases}$$

where z is in meters. In this example the frequency of operation is 3 GHz, wind speed Ws = 0, transmitter height = 30m, and Z_{max} = 512m. We choose N = 512, resulting in a vertical step size Δz = 2m, and choose a horizontal step size Δx = 200m. Figure 12 shows the Propagation Factor versus Receiver Height, at a range of 40 km. As for the case of a standard atmosphere, the propagation characteristics for the tri-linear duct are in agreement with Kuttler and Dockery [3].

C. CASE 3 - EVAPORATION DUCT

The next refractivity profile we investigate is that of an evaporation duct as depicted in Figure 13. The numerical values for the evaporation duct are shown in Table 1.

Table 1. Refractivity Data For Evaporation Duct

Height (m)	M(z)
0.000	340.00
0.135	323.00
0.223	321.76
0.368	320.53
0.607	319.31
1.000	318.11
1.649	316.94
2.718	315.83
4.482	314.80
7.389	313.91
12.182	313.26
20.000	312.99
33.115	313.38
54.598	314.81
90.017	317.99
148.413	324.04
165.000	325.76
300.000	339.745

Figures 14 and 15 illustrate that by wisely choosing the value of the upper boundary, accurate data can be obtained where it may not have been otherwise possible. Figure 14 shows propagation in an evaporation duct with Z_{max}=75m, N=512, transmitter and receiver height = 25m, and frequency=10 GHz. At the longer ranges the effects of the upper boundary and the evaporation duct prevent the PF from decaying in a stable manner. By increasing the upper boundary to 150m and N=1024 and keeping all others parameters the same, Figure 15 shows a stable PF can be achieved even at the longer ranges.

D. EVAPORATION DUCT WITH ROUGH SEA SURFACE

In this example we consider the same evaporation duct as above, but now we add the effects of a rough ocean surface. The wind speed considered is 10 m/s which results in a wave height of 0.51m from (11). Figure 16 shows both the propagation factors for a signal

in the evaporation duct with no wind Ws = 0 m/s and for Ws = 10 m/s. Other data are Z_{max} = 150m, frequency = 10 GHz and N = 1024. The effects of a rough ocean surface are more pronounced than the case of standard atmosphere. Specifically we see, (i) a reduction of the specular component as seen by the smaller excursions of the rough sea PF in the interference region, and (ii) increased losses for the rough sea PF over the smooth sea PF at greater distances. Figure 17 gives the results for PF vs. Receiver Height for the evaporation duct at a range of 100 km for wind speeds of 0 m/s, 10 m/s and 20 m/s. The upper boundary is Z_{max} = 300m, frequency of operation = 10 GHz, N=2048, and transmitter height z_t = 25m. This figure illustrates the overall reduction in PF as surface roughness increases, however it also shows significant variation in the value of PF with respect to height due to the effect of the evaporation duct.

E. CASE 4 - SURFACE DUCT

The last example to be considered is the case of propagation in a surface duct. This refractivity is depicted in Figure 18 and its numerical form is given by :

$$M(z) = \begin{cases} 350 - 0.335z & 0 \le z \le 45.7 \\ 329.36 + 0.1164z & z > 45.7 \end{cases}$$

Figure 19 shows the Propagation Factor vs. Range out to a range of 100 km for a signal traveling in the surface duct over smooth and rough ocean surfaces (Ws = 0 m/s and Ws = 10 m/s). The frequency of operation is 10 GHz, transmitter and receiver height $z_t = 25\text{m} = z_r$, and an upper boundary Z_{max} = 150m. As in the previous example, Figure 19 illustrates that the rough ocean surface generally decreases the propagation factor as wind speed increases. The last example considered is Propagation Factor vs Receiver Height at a range of 100km for the surface duct with an upper boundary Z_{max} = 300m. The results are shown in Figure 20 with all parameters remaining the same as the previous case except here

N = 2048. Once again surface roughness has reduced the propagation factor, and the effect of the surface duct has resulted in variations of the PF as receiver height is changed.

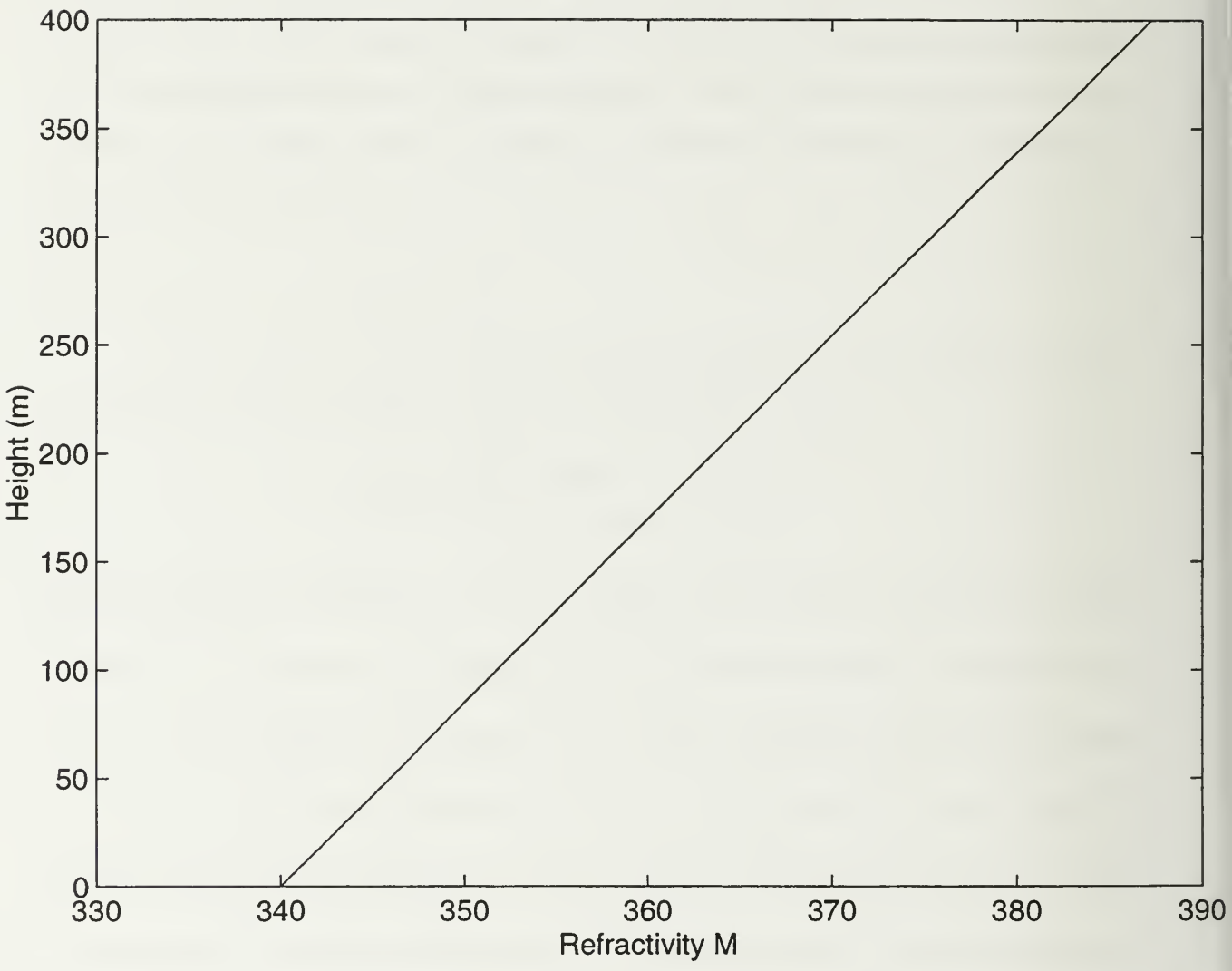

Figure 5. Refractivity for Standard Atmosphere.

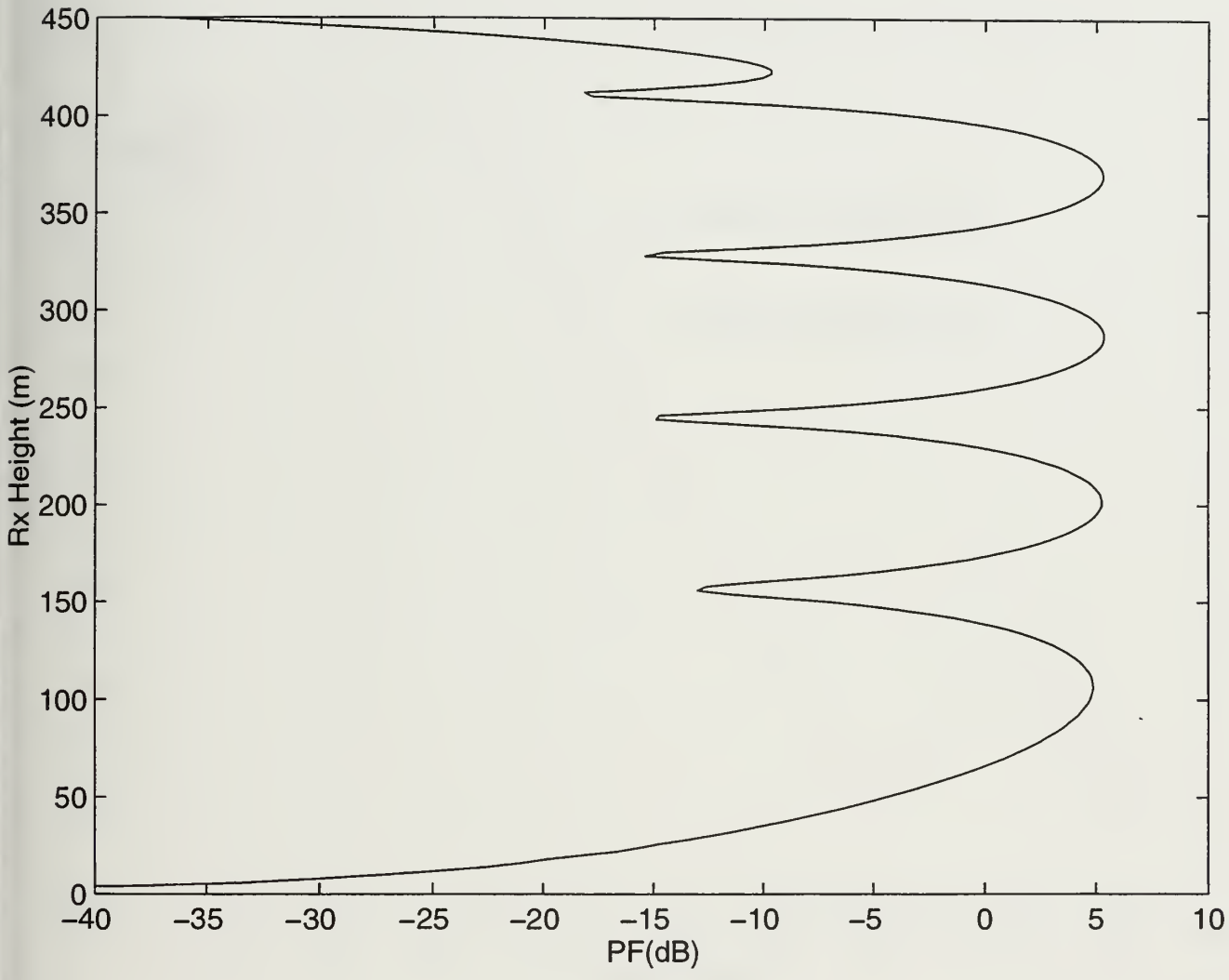

Figure 6. PF vs. Receiver Height for standard atmosphere at range of 40 km. Transmitter height z_t = 30m, wind speed Ws = 0, frequency = 3 GHz, N = 512, vertical polarization and omnidirectional antenna.

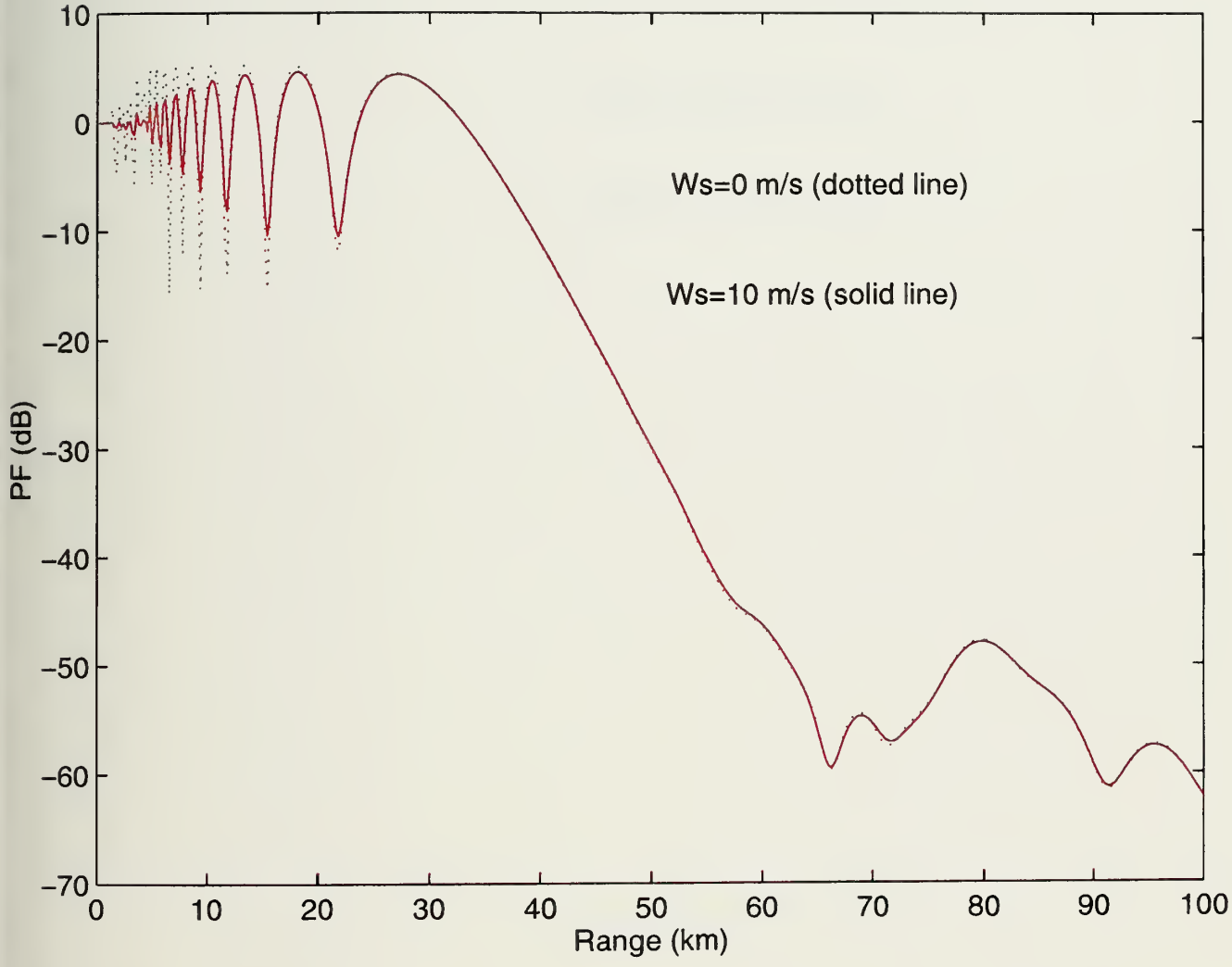

Figure 7. **Smooth and rough sea (Ws = 10 m/s) PF vs. Range for standard atmosphere out to a range of 100 km with upper boundary Z_{max} = 150m. Transmitter height z_t = 25m, receiver height z_r = 25m, frequency = 10 GHz, N = 1024, vertical polarization and omnidirectional antenna.**

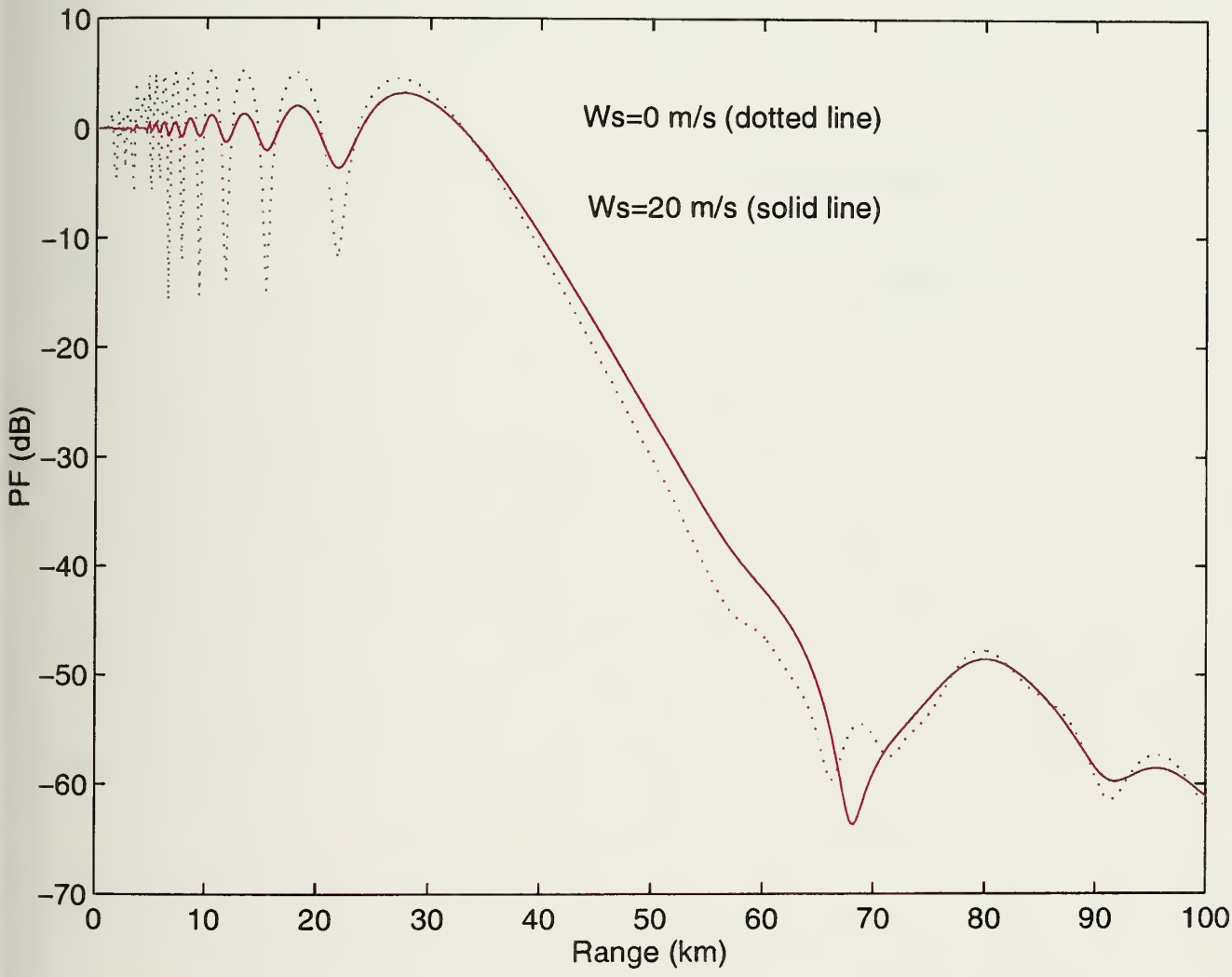

Figure 8. **Smooth and rough sea (Ws = 20 m/s) PF vs. Range for standard atmosphere out to a range of 100 km with upper boundary Z_{max} = 150m. Transmitter height z_t = 25m, receiver height z_r = 25m, frequency = 10 GHz, N = 1024, vertical polarization and omnidirectional antenna.**

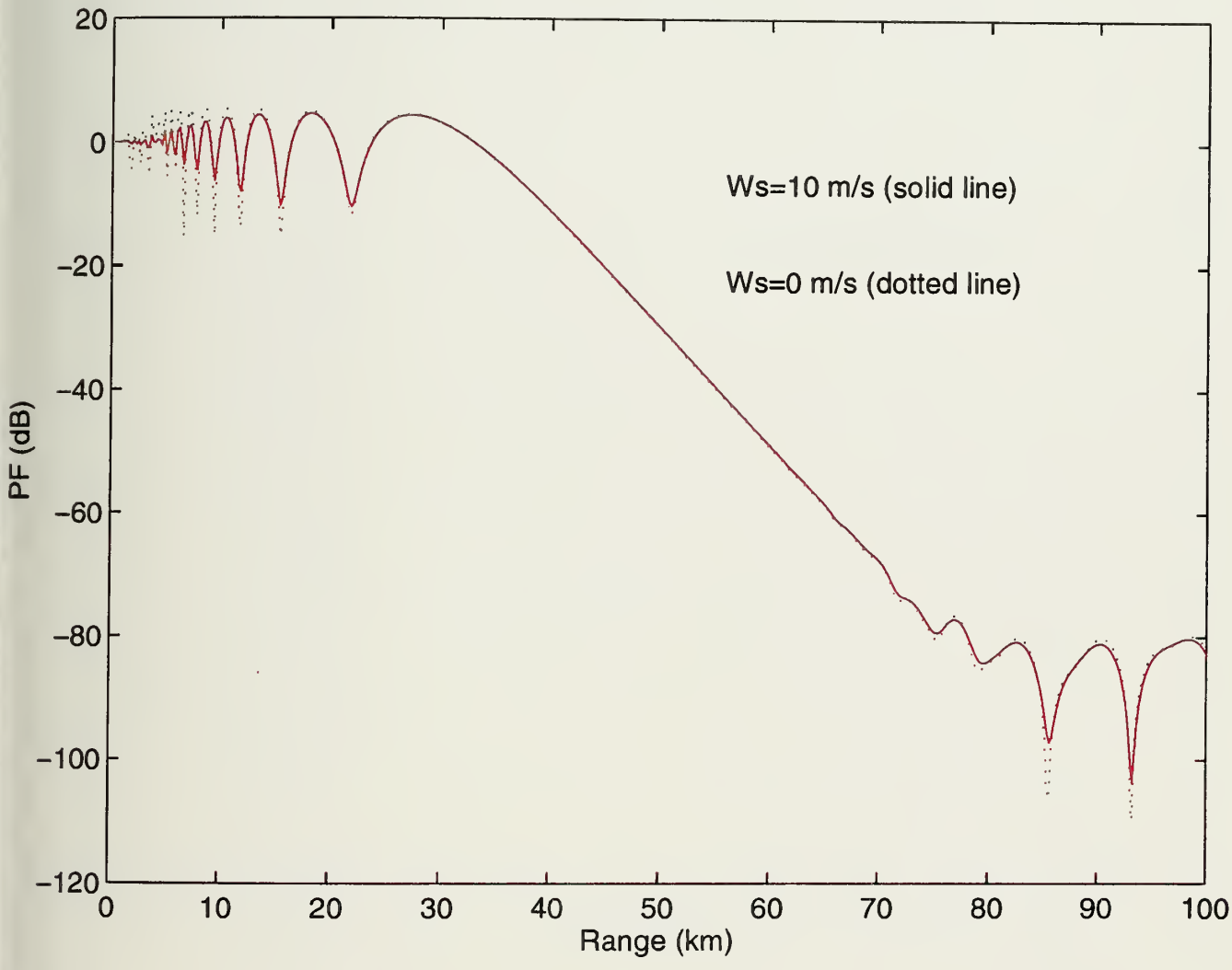

Figure 9. **Smooth and rough sea (Ws = 10 m/s) PF vs. Range for standard atmosphere out to a range of 100 km with upper boundary Z_{max} = 300m. Transmitter height z_t = 25m, receiver height z_r = 25m, frequency = 10 GHz, N = 2048, vertical polarization and omnidirectional antenna.**

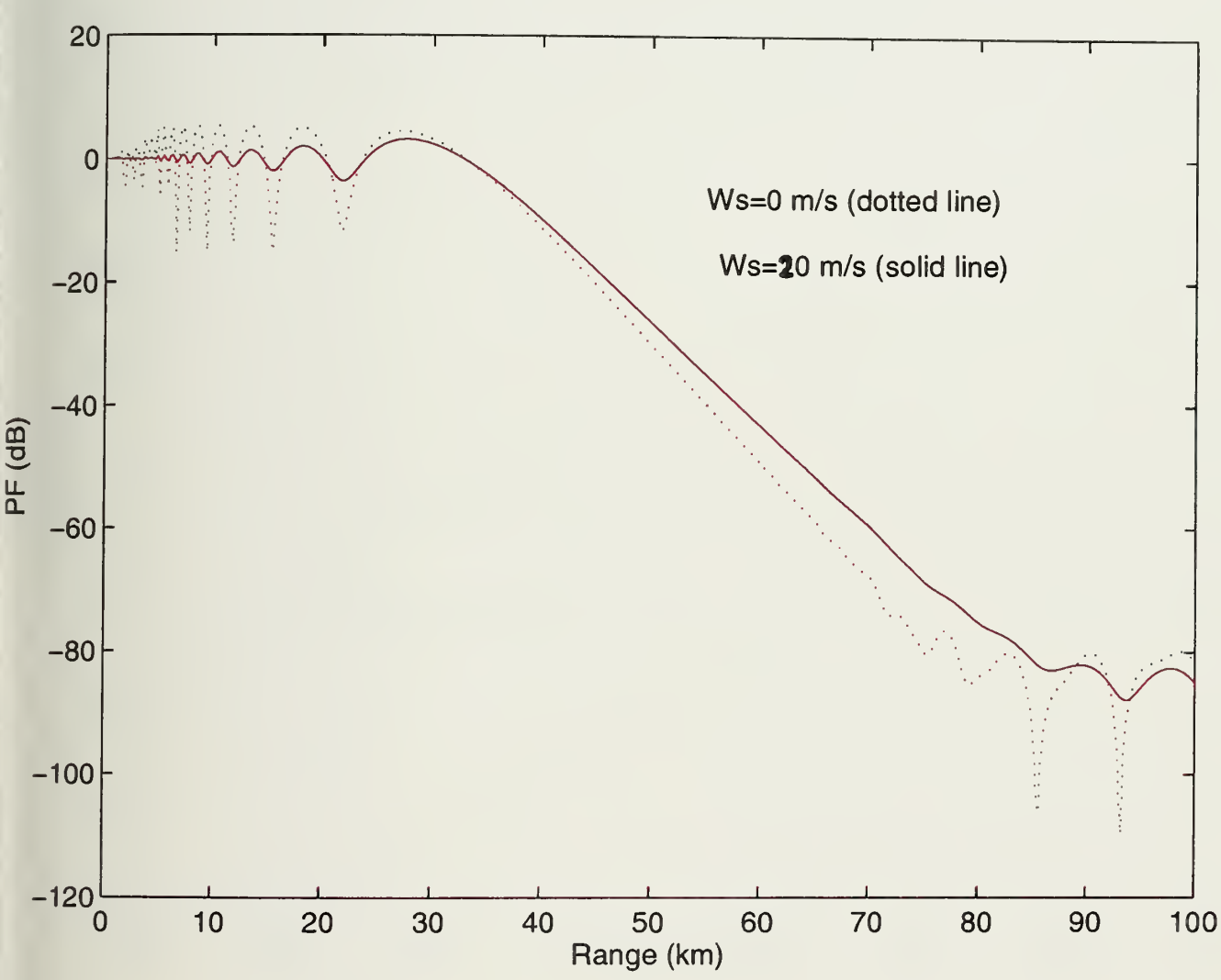

Figure 10. Smooth and rough sea (Ws = 20 m/s) PF vs. Range for standard atmosphere out to a range of 100 km with upper boundary Z_{max} = 300m. Transmitter height z_t = 25m, receiver height z_r = 25m, frequency = 10 GHz, N = 2048, vertical polarization and omnidirectional antenna.

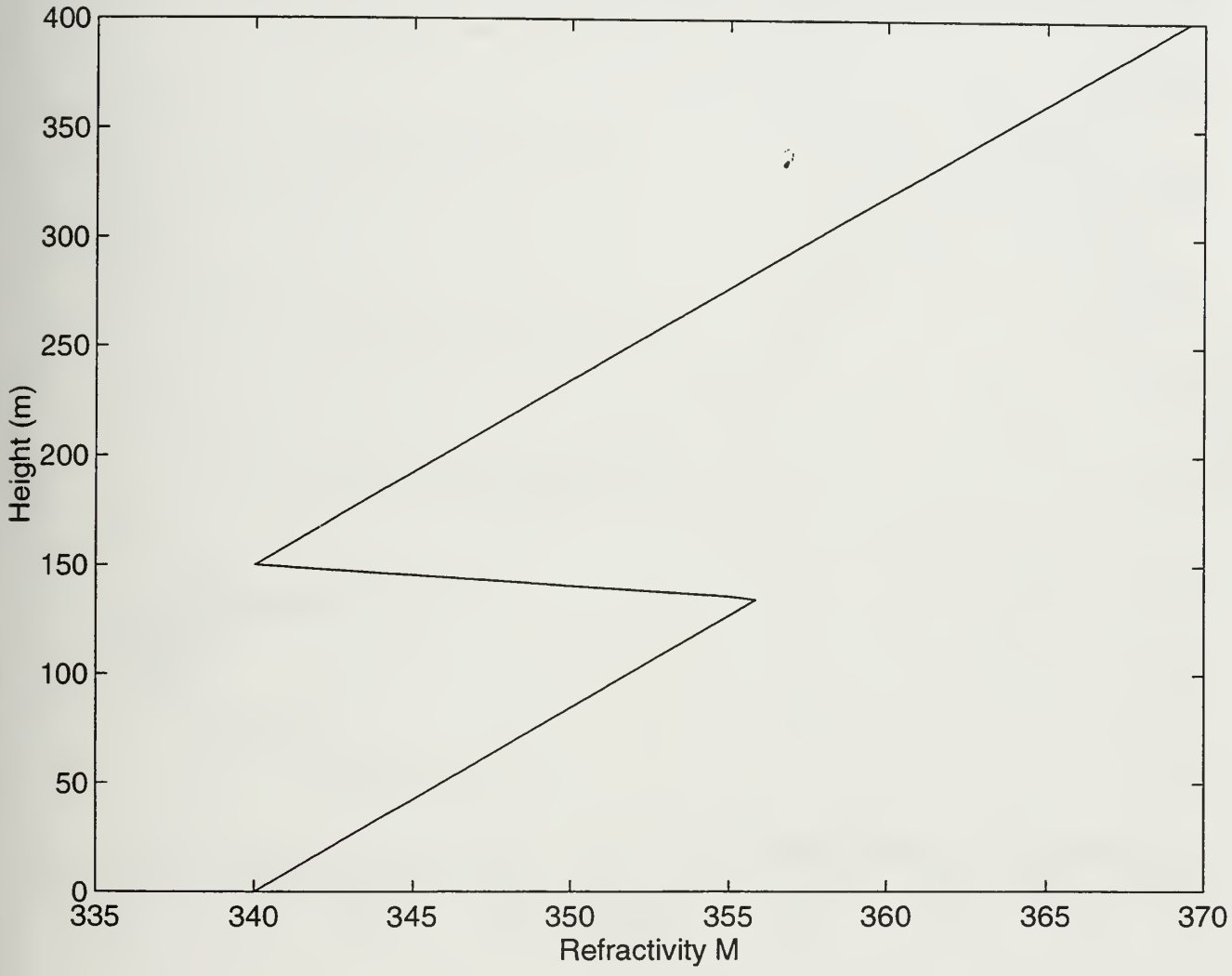

Figure 11. Refractivity for Tri-Linear Duct

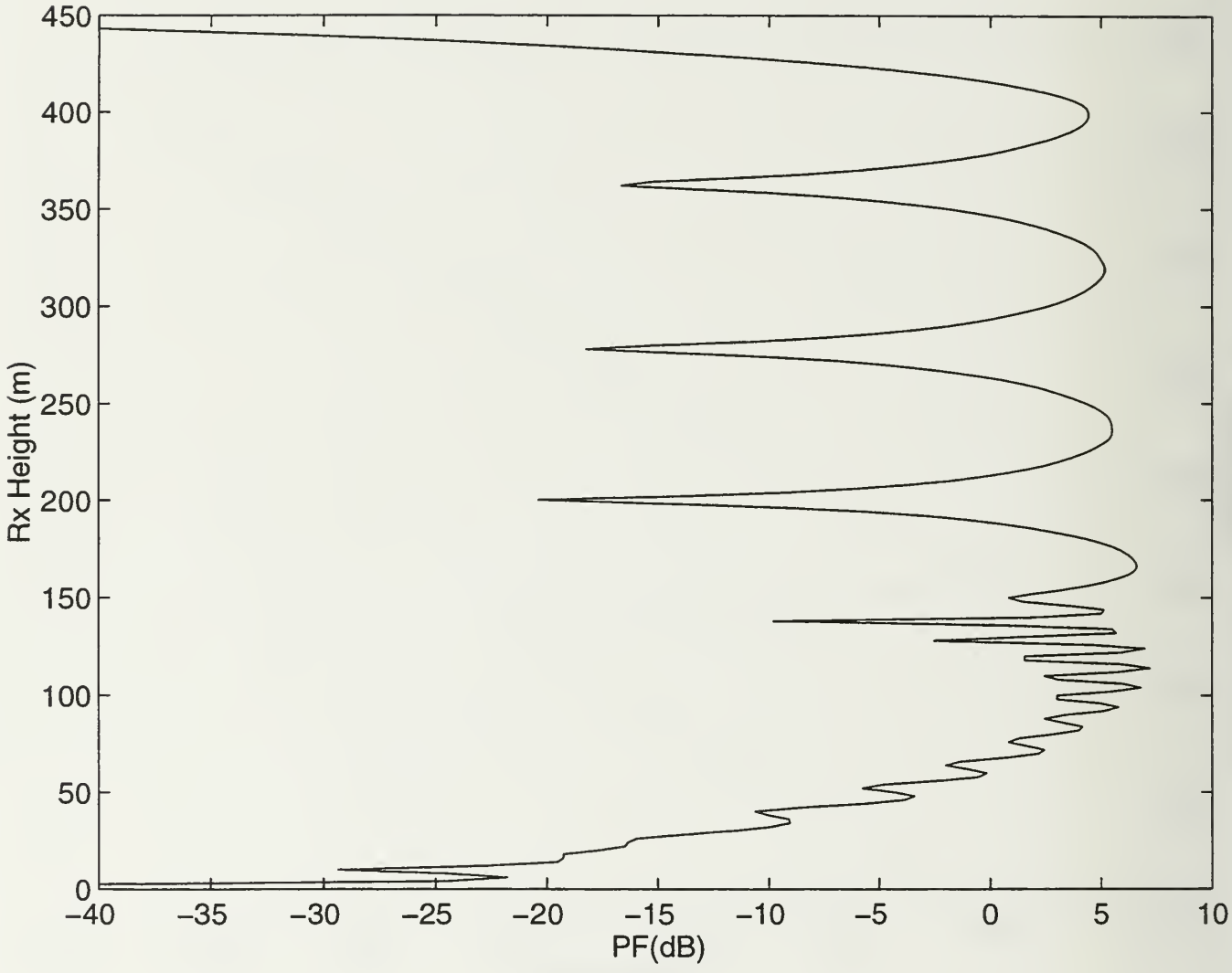

Figure 12. PF vs. Receiver Height for tri-linear duct at range of 40 km. Transmitter height z_t = 30m, wind speed Ws = 0, frequency = 3 GHz, N = 512, vertical polarization and omnidirectional antenna.

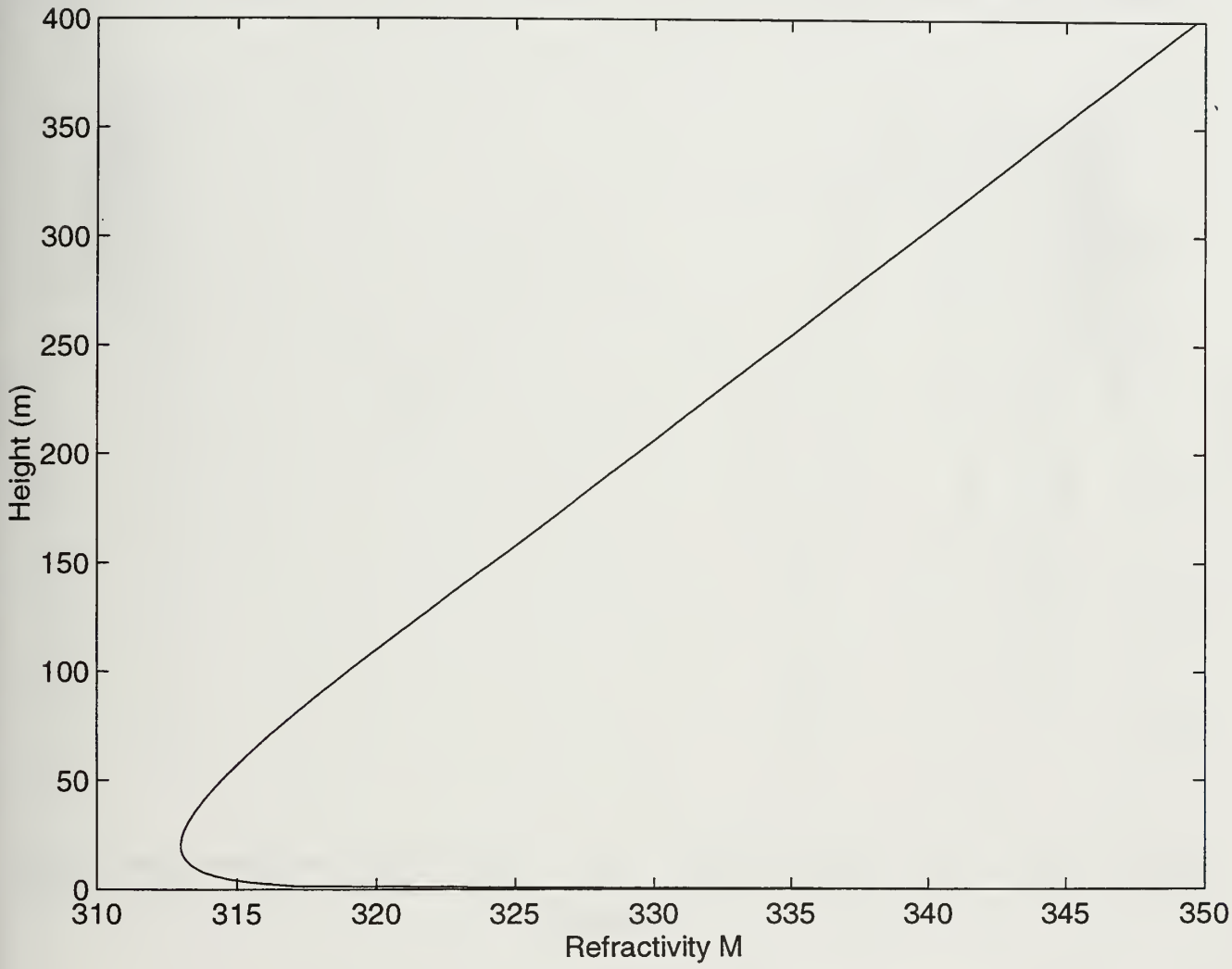

Figure 13. Refractivity for Evaporation Duct.

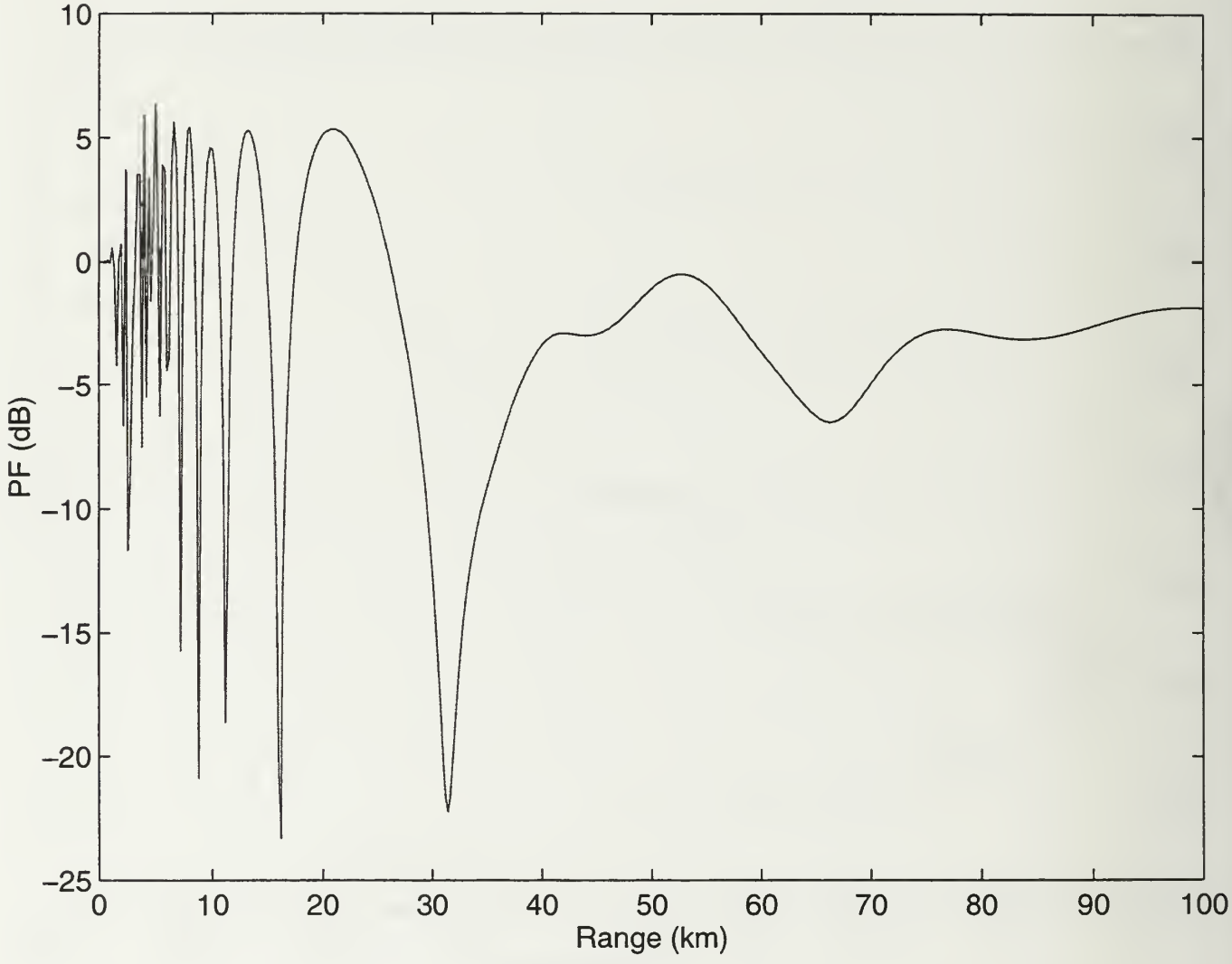

Figure 14. PF vs. Range for evaporation duct to a range of 100 km with upper boundary Z_{max} = 75m. Transmitter height z_t = 25m, receiver height z_r = 25m, frequency = 10 GHz, wind speed Ws = 0, N = 512, vertical polarization and omnidirectional antenna.

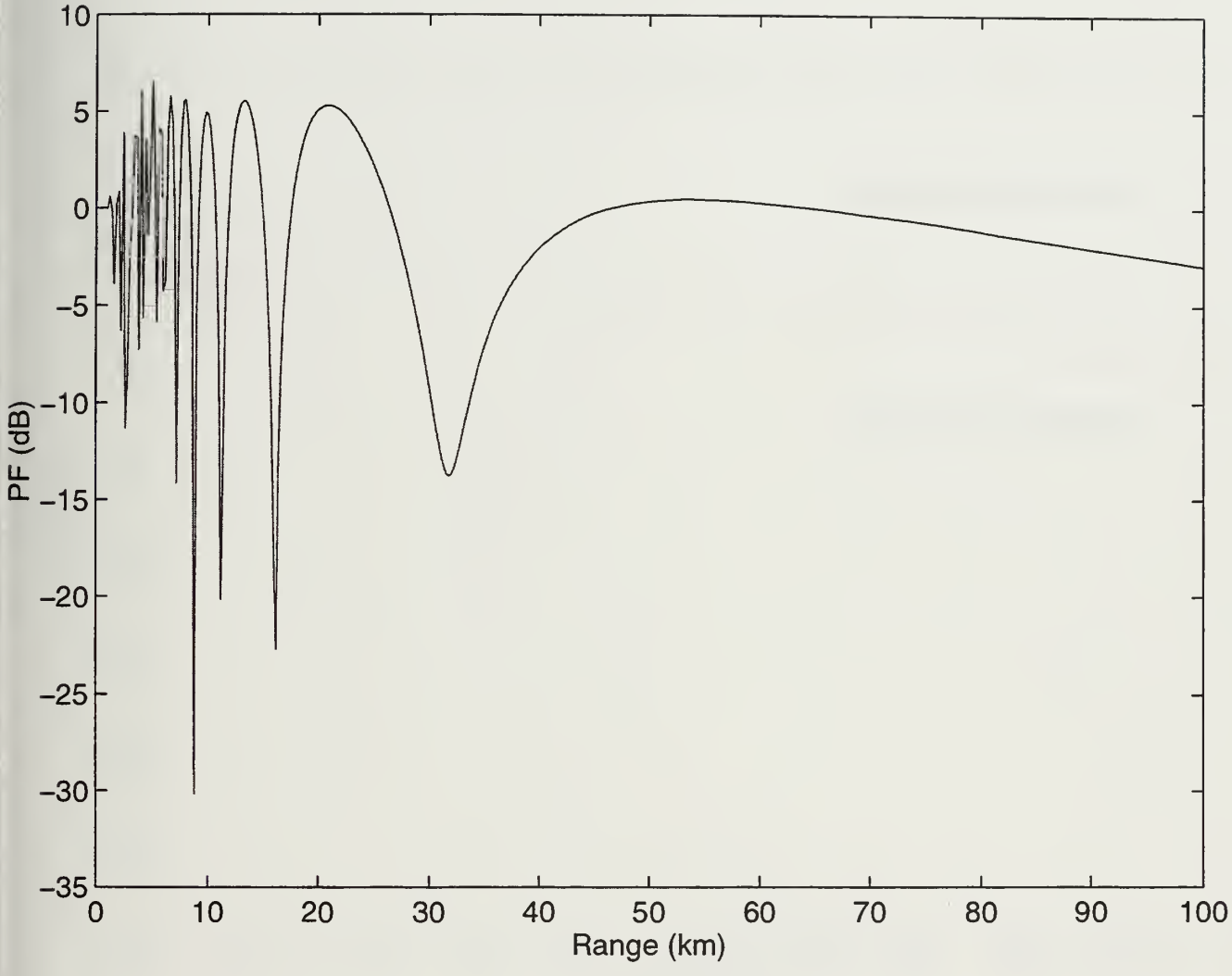

Figure 15. PF vs. Range for evaporation duct to a range of 100 km with upper boundary Z_{max} = 150m. Transmitter height z_t = 25m, receiver height z_r = 25m, frequency = 10 GHz, wind speed Ws = 0, N = 1024, vertical polarization and omnidirectional antenna.

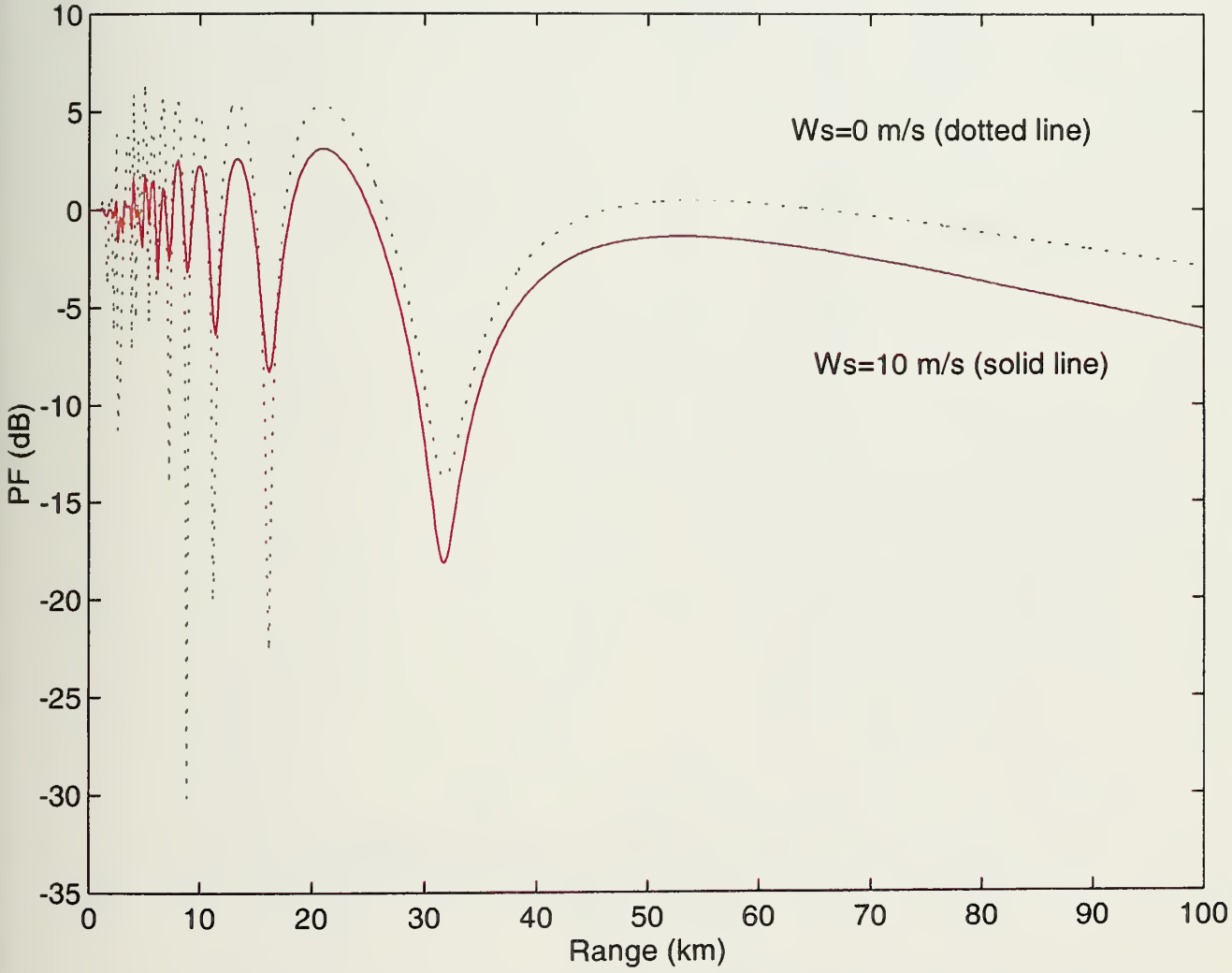

Figure 16. Smooth and rough sea (WS = 10 m/s) PF vs. Range for evaporation duct to a range of 100 km with upper boundary Z_{max} = 150m. Transmitter height z_t = 25m, receiver height z_r = 25m, frequency = 10 GHz, wind speed = 0 m/s, N = 1024, vertical polarization and omnidirectional antenna.

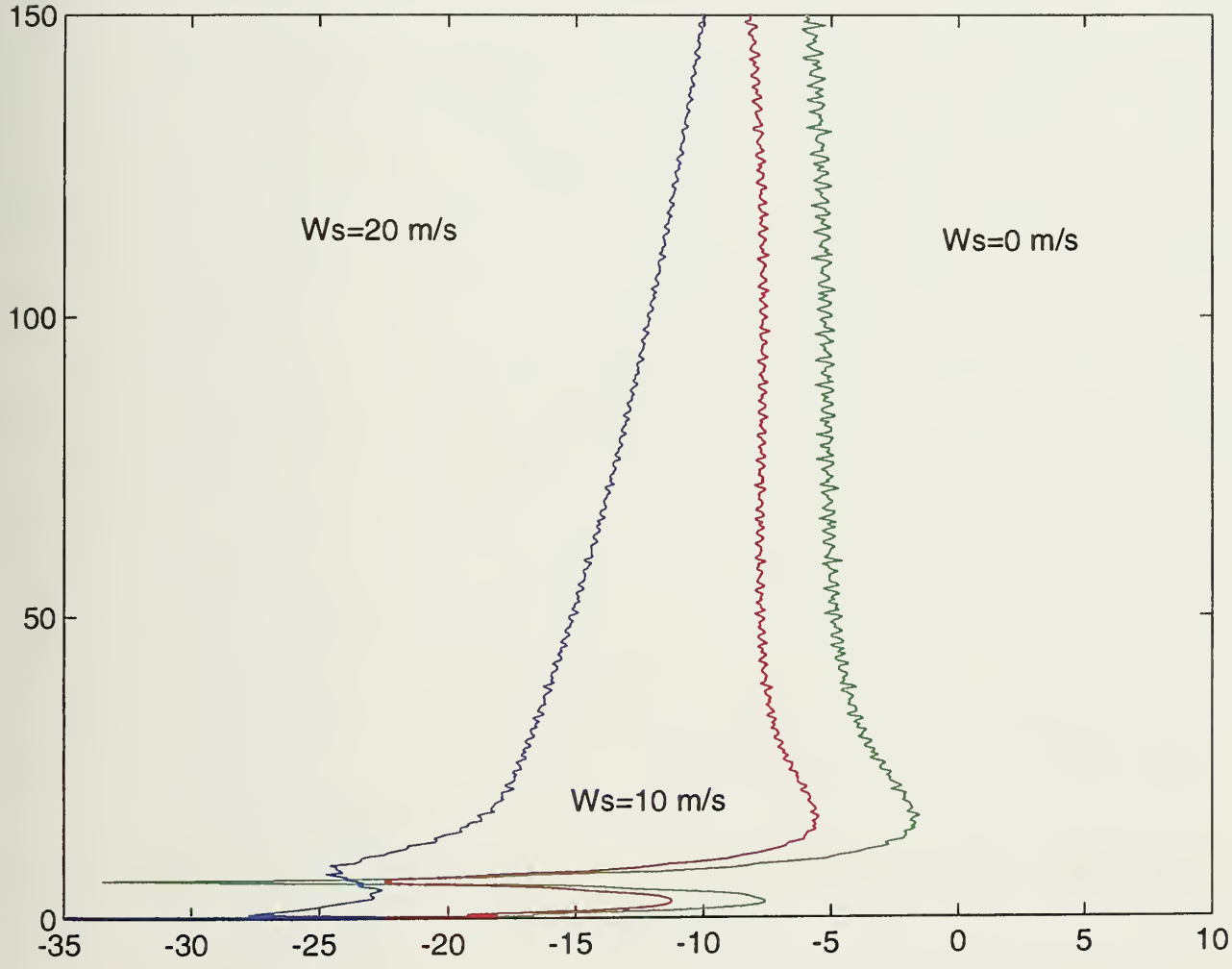

Figure 17. PF vs. Range for evaporation duct to a range of 100 km with wind speed = 0 m/s, 10 m/s, 20 m/s. Upper boundary Z_{max} = 300m, transmitter height z_t = 25m, receiver height z_r = 25m, frequency = 10 GHz, N = 2048, vertical polarization and omnidirectional antenna.

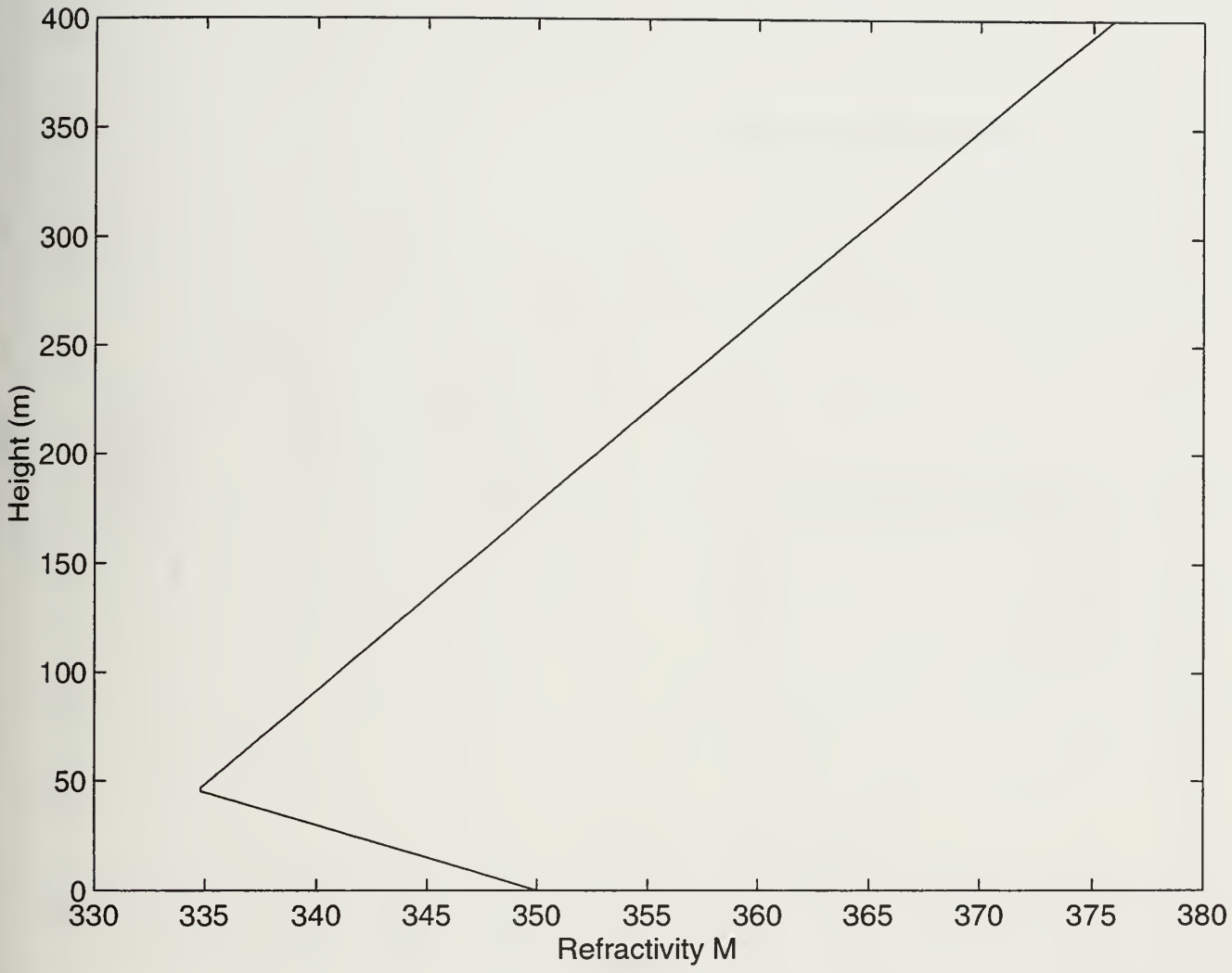

Figure 18. Refractivity for Surface Duct.

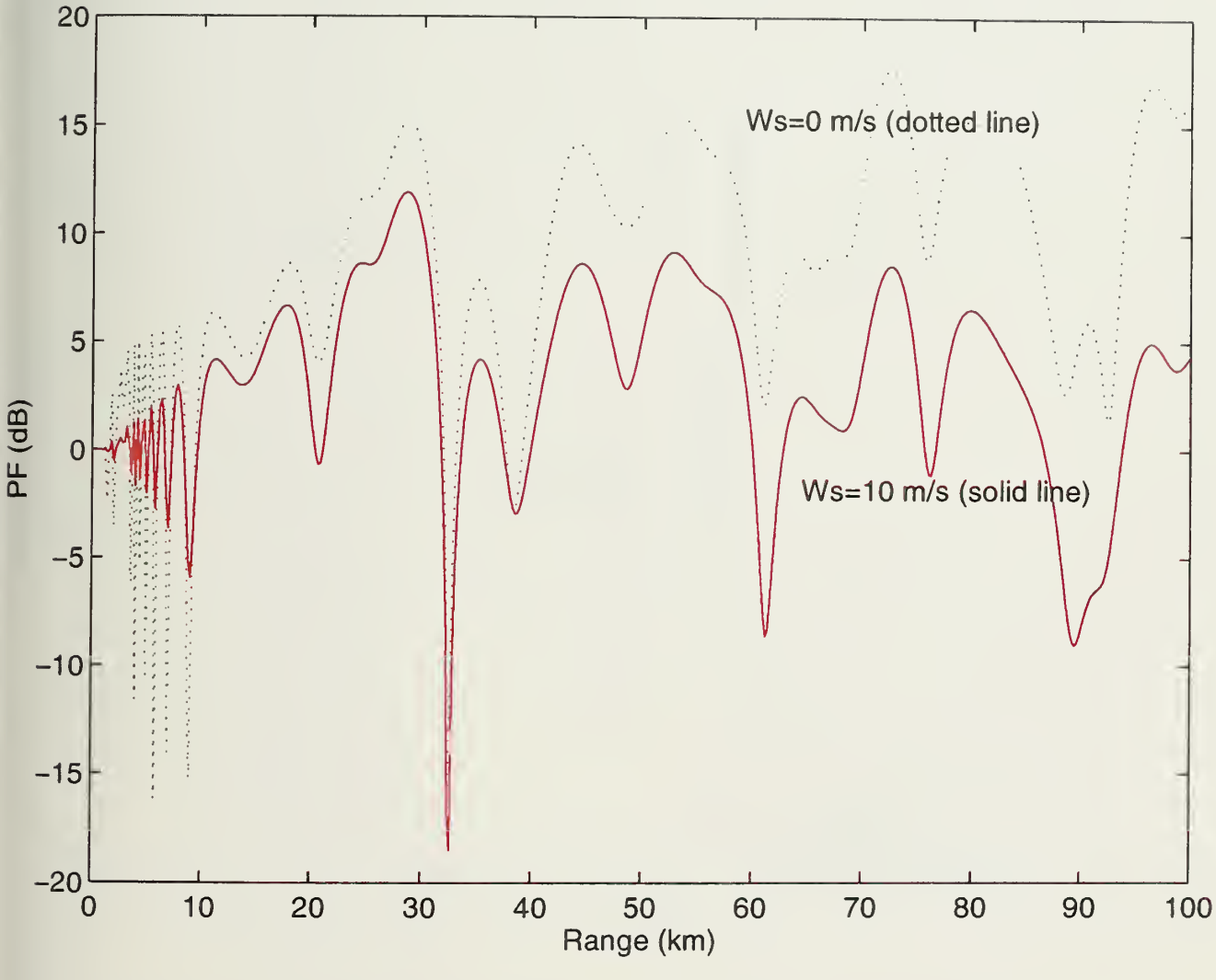

Figure 19. Smooth and rough sea (WS = 10 m/s) PF vs. Range for surface duct out to a range of 100 km with upper boundary Z_{max} = 150m. Transmitter height z_t = 25m, receiver height z_r = 25m, frequency = 10 GHz, wind speed Ws = 0 m/s, N = 1024, vertical polarization and omnidirectional antenna.

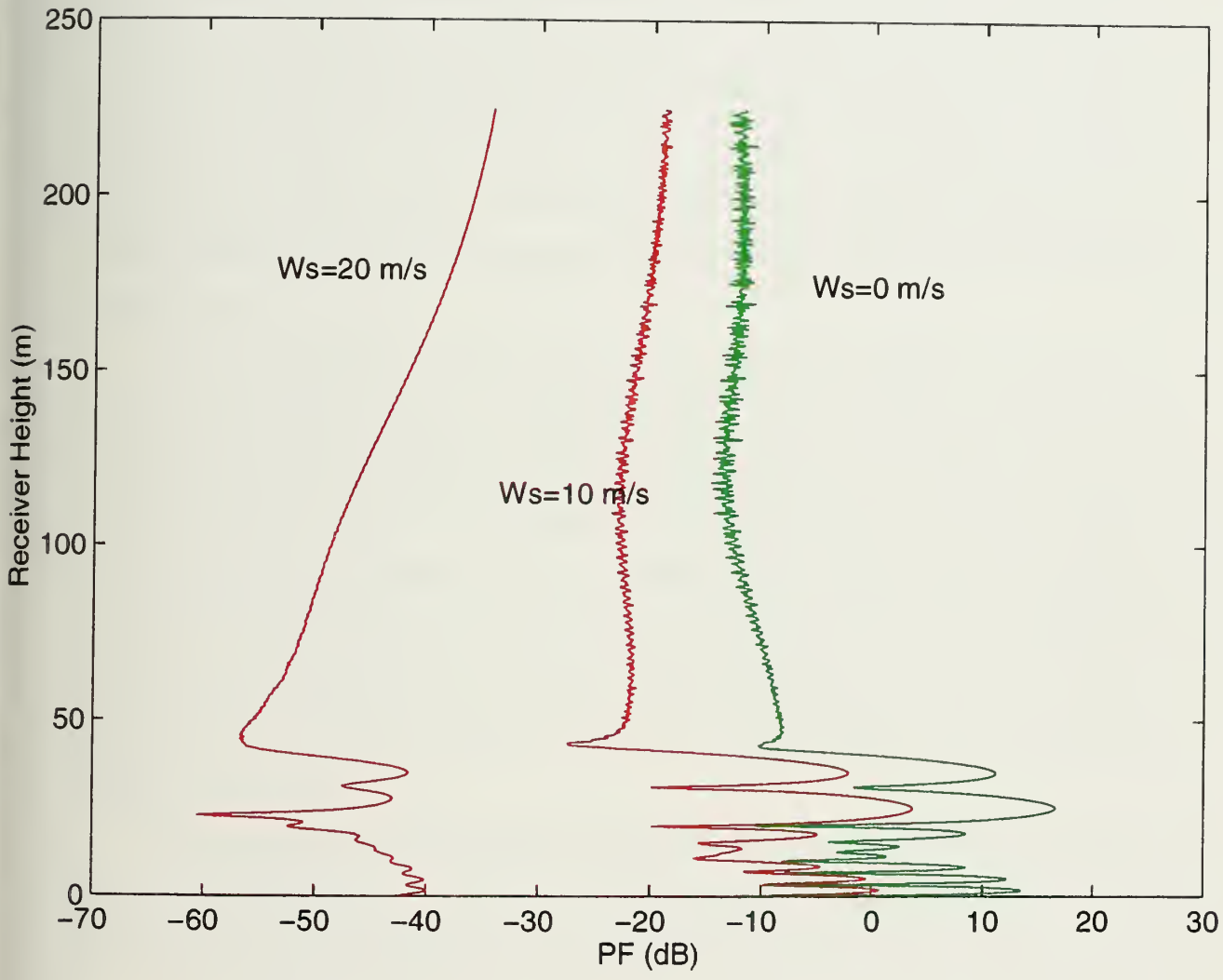

Figure 20. PF vs. Receiver Height for evaporation duct at a range of 100 km with wind speeds Ws = 0 m/s, 10 m/s and 20 m/s. Upper boundary Z_{max} = 300m. Transmitter height z_t = 25m, receiver height z_r = 25m, frequency = 10 GHz, N = 2048, vertical polarization and omnidirectional antenna.

V. CONCLUSIONS

In this thesis, a method of predicting radiowave propagation of vertically polarized waves over rough ocean surfaces was implemented and tested. An efficient solution was made possible by only considering one way propagation, thus allowing us to use the split-step parabolic equation method to tackle our problem instead of the much more computationally intensive Helmholtz equation. Our method incorporates the contributions from direct and reflected waves at any distance downrange from the transmitter, but ignores the effects of backscattering. This allowed us to develop a range stepping technique to determine the strength of the propagating waves. The fact that the split-step technique involves Fourier kernels (plane waves) made it possible to incorporate the effects of sea surface roughness directly into the spectral domain through the use of a rough surface reduction factor.

The main purpose of this thesis was to modify the equations developed by Janaswamy [1] so the propagation of vertically polarized waves could also be solved by the split-step PE method. Numerical results for the case of vertical polarization show great similarity with those described in that report for the various refractivity profiles examined. The effects of the upper boundary layer are a significant factor in the accuracy of our model and must be taken into consideration when interpreting data. The user must take into consideration the value of the upper boundary, surface roughness and vertical step size as determined by the number of points, N, used in the FFT, to ensure accurate results are obtained with this model.

The model presented in this thesis is applicable to propagation predictions for areas such as communications and radar. It is a useful tool for those designing, developing, and deploying new systems and for those that may be analyzing systems already in use.

LIST OF REFERENCES

1. Janaswamy, R., "A Rigorous Way of Incorporating Sea Surface Roughness Into the Parabolic Equation," Tech. Rep. NPS-EC-95-008, Naval Postgraduate School, Monterey, California, September 1995.

2. Miller, A. R., et al., "New Derivation of Rough Surface Reflection Coefficient and for the Derivation of Sea-wave Elevations," *IEE Proc.*, Vol. 131, no. 2, pp. 114-116, April 1984.

3. Kuttler, J. R., and G. D. Dockery, "Theoretical Description of the Parabolic Approximation/Fourier Split-step Method of Representing Electromagnetic Propagation in the Troposphere," *Radio Science*, Vol. 26, no. 2, pp. 153-162, March-April 1991.

4. Tappert, F. D., "The Parabolic Approximation Method," in *Wave Propagation and Underwater Acoustics*, (Lecture Notes in Physics), J. B. Keller and J. S. Papadakis, Eds., New York: Springer-Verlag, Vol. 70, 1977.

5. Beckmann, P., and A. Spizzichino, *The Scattering of Electromagnetic Waves From Rough Surfaces,* Norwood, Massachusetts: Artech House, Inc., 1987.

6. Report 1008-1 "*Reflections From the Surface of the Earth*," Vol. V of Recommendations and Reports of the CCIR, XVIIth Planery Assembly, ITU, Geneva, 1990.

7. Papoulis, A., *The Fourier Integral and its Applications*, New York: McGraw Hill, 1962.

INITIAL DISTRIBUTION LIST

No. Copies

1. Defense Technical Information Center 2
   8725 John J. Kingman Rd., STE 0944
   Ft. Belvoir, VA 22060-6218

2. Dudley Knox Library 2
   Naval Postgraduate School
   411 Dyer Rd.
   Monterey, CA 93943-5101

3. Chairman, Code EC 1
   Department of Electrical and Computer Engineering
   Naval Postgraduate School
   Monterey, CA 93943-5101

4. Professor Ramakrishna Janaswamy 2
   Code EC/Js
   Naval Postgraduate School
   Monterey, CA 93943-5102

5. Professor David C. Jenn 1
   Code EC/Jn
   Naval Postgraduate School
   Monterey, CA 93943-5102

6. Mr. Kenneth Anderson 1
   NCCOSC RDTE DIV 883
   53560 Hull Street
   San Diego, CA 92152-5001

7. Ms. Amalia Barios 1
   NCCOSC RDTE DIV 883
   53560 Hull Street
   San Diego, CA 92152-5001

8. Mr. Herbert Hitney 1
NCCOSC RDTE DIV 883
53560 Hull Street
San Diego, CA 92152-5001

9. Mr. Richard Paulus 1
NCCOSC RDTE DIV 883
53560 Hull Street
San Diego, CA 92152-5001

10. LCDR Jeffrey G. Conrad 2
1547 Delia Cresent
Orleans, Ontario,
Canada
K4A 2Y1